



HAL
open science

Numerical modelling of the lithiation of silicon nanoparticles in lithium-ion batteries

Guilherme Dalevedo Viana, Renaud Masson, Bruno Michel, Benoit Mathieu,
M. Găărăjeu

► **To cite this version:**

Guilherme Dalevedo Viana, Renaud Masson, Bruno Michel, Benoit Mathieu, M. Găărăjeu. Numerical modelling of the lithiation of silicon nanoparticles in lithium-ion batteries. Congrès Français de Mécanique, Association Française de Mécanique (AFM), Aug 2022, Nantes, France. hal-03888588

HAL Id: hal-03888588

<https://hal.science/hal-03888588v1>

Submitted on 7 Dec 2022

HAL is a multi-disciplinary open access archive for the deposit and dissemination of scientific research documents, whether they are published or not. The documents may come from teaching and research institutions in France or abroad, or from public or private research centers.

L'archive ouverte pluridisciplinaire **HAL**, est destinée au dépôt et à la diffusion de documents scientifiques de niveau recherche, publiés ou non, émanant des établissements d'enseignement et de recherche français ou étrangers, des laboratoires publics ou privés.

Numerical modelling of the lithiation of silicon nanoparticles in lithium-ion batteries

Guilherme Dalevedo^{1,3}, Renaud Masson¹, Bruno Michel¹, Benoit Mathieu², Mihail Garajeu³



¹CEA DES, IRESNE, DEC, SESC, Cadarache, 13108 Saint-Paul-lez-Durance, France

²CEA, DRT, LITEN, DEHT/SAMA 38000 Grenoble, France

³Aix Marseille Université, CNRS, Centrale Marseille, LMA, F-13453 Marseille, France

DE LA RECHERCHE À L'INDUSTRIE



CFM 2022

1st September

IRESNE | DEC | SESC | LM2C

Institut de recherche sur les systèmes nucléaires pour la production d'énergie bas carbone

Context :

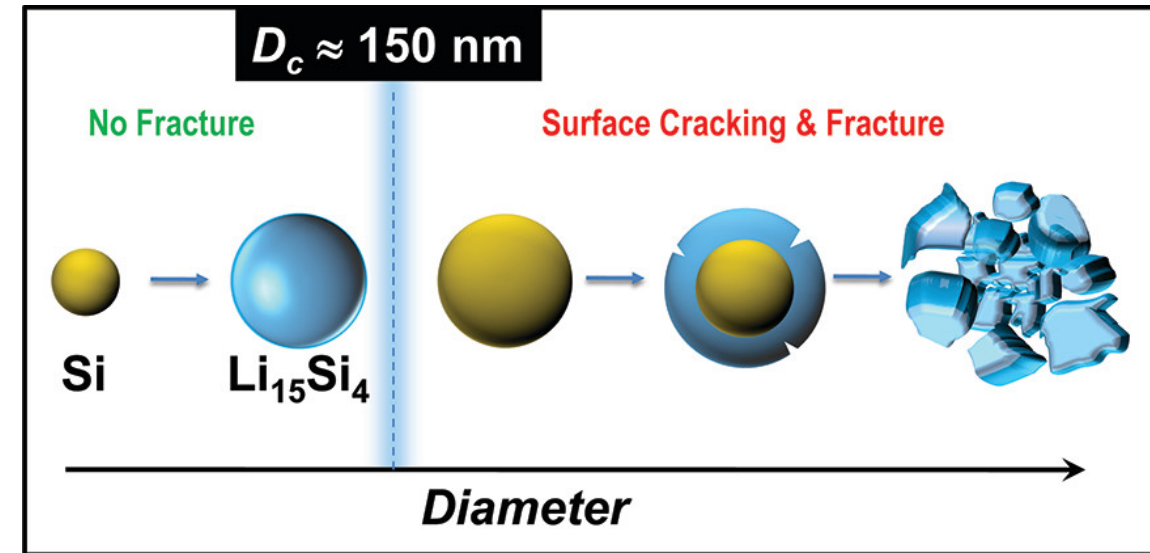
Why silicon material ?

High specific capacity (4200 mAh/g) , reasonable price, abundance in nature.

Disadvantages: very important swelling during the charge/discharge of Lithium (lithiation) which can lead to the degradation of the electrode.

Mitigation:

- Decreasing the size of the silicon particles to the nanoscale (20 - 200 nm).
- Use of a coating to limit the expansion of the silicon particles (buffer).



Liu et al. 2012

Context :

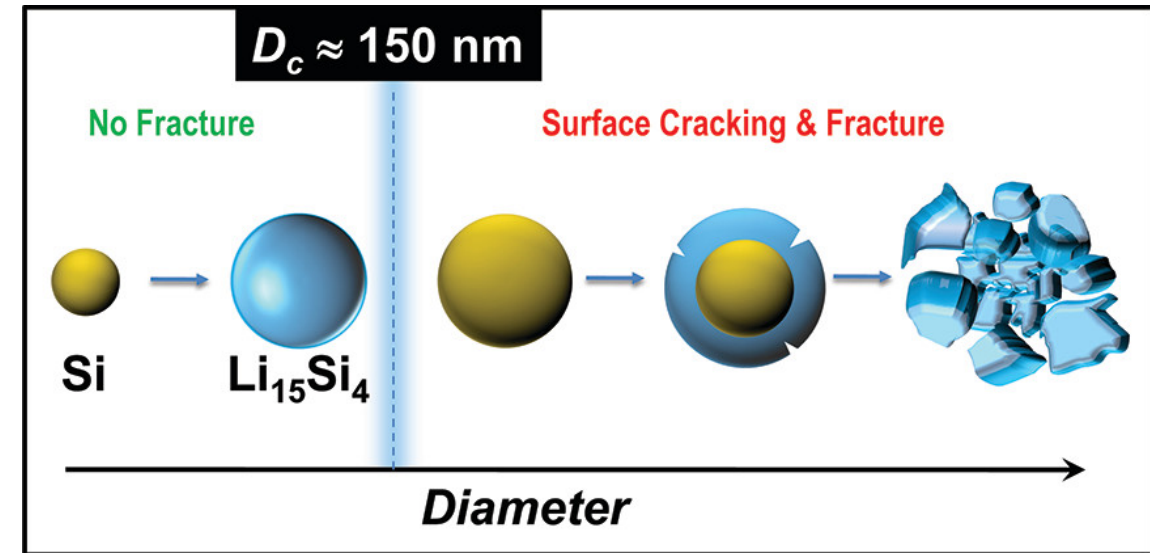
Why silicon material ?

High specific capacity (4200 mAh/g) , reasonable price, abundance in nature.

Disadvantages: very important swelling during the charge/discharge of Lithium (lithiation) which can lead to the degradation of the electrode.

Mitigation:

- Decreasing the size of the silicon particles to the nanoscale (20 - 200 nm).
- Use of a coating to limit the expansion of the silicon particles (buffer).

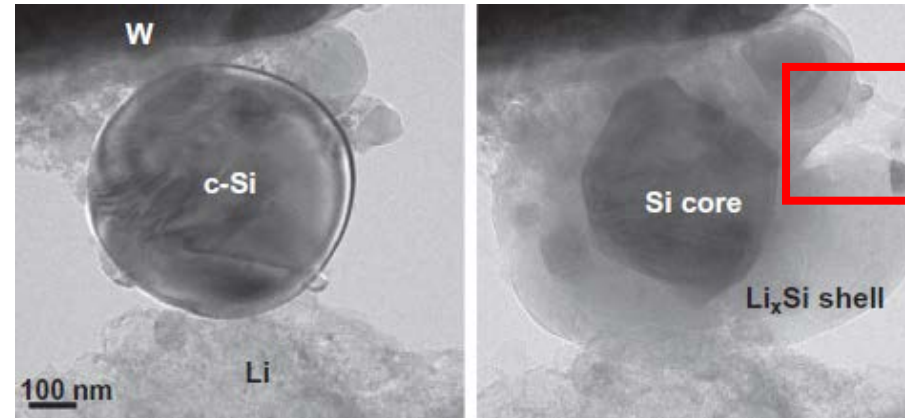
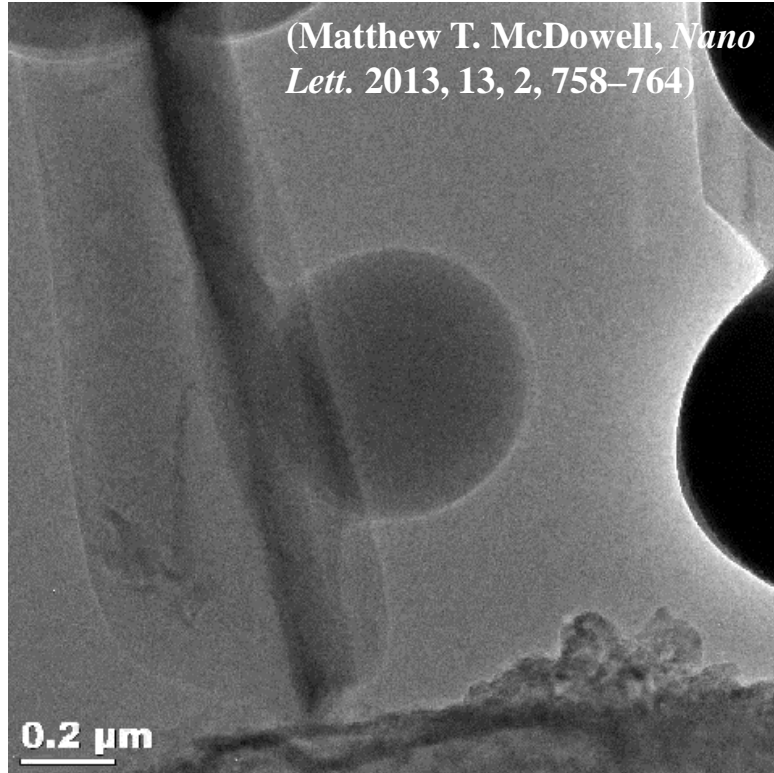


Liu et al. 2012

Objectives of this work:

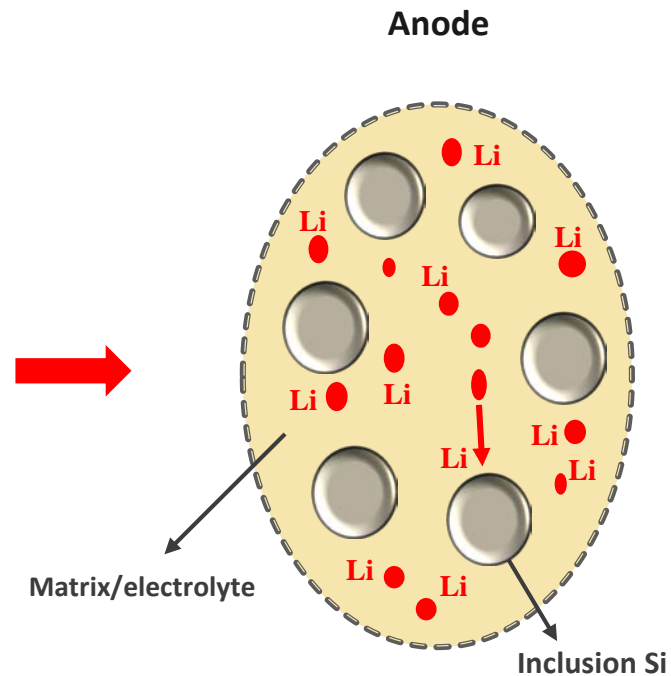
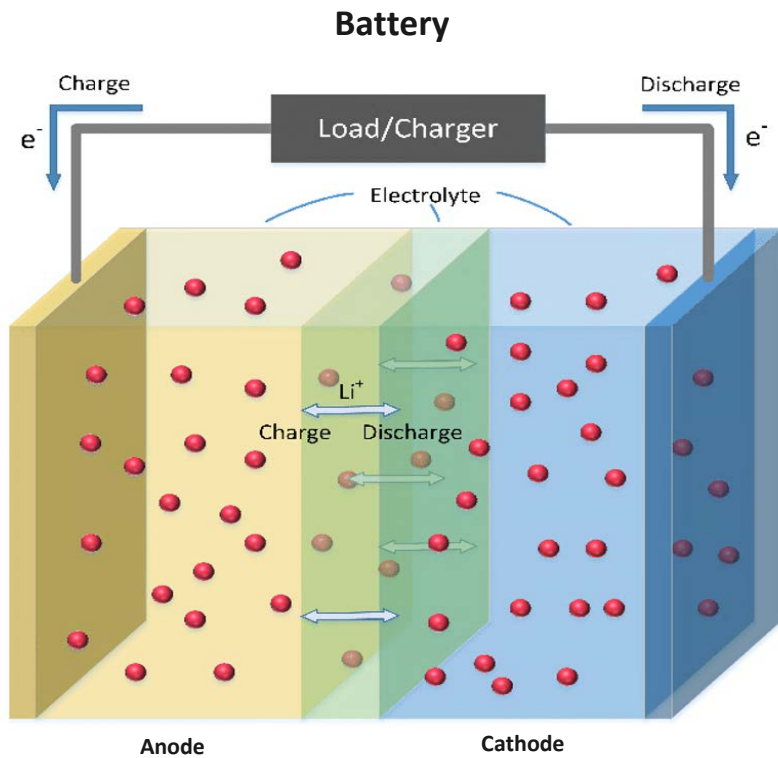
- Understanding and modeling of the mechanical effects of lithiation of a silicon particle. ✓
- Validation of the model with experimental measurements (example: XRD measurement). ⌚
- Study by simulation of technological solutions : coating, microparticles. ⌚

Experimental observations: lithiation of a free silicon particle



- Formation of an amorphization front between the two phases (1 nm).
- Formation of two phases during lithiation: a lithium rich shell (Li_xSi) and a pure silicon core (pristine) : $3.75 \text{ Li} + \text{c-Si} = \text{Li}_{3.75}\text{Si}$
- Fracture of the particle periphery.

Context :



Assumptions:



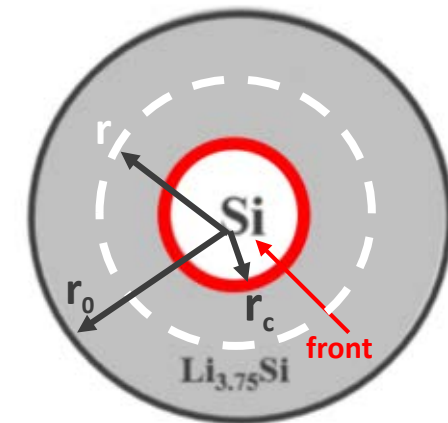
- Spherical geometry for inclusion.
- Mechanical - diffusion coupling (similar to a thermomechanical problem).
- Soft matrix/electrolyte : no effect on the mechanics of the particle.
- Isotropic lithiation of the particle.

Consequence:

- Problem reduces to 1D.

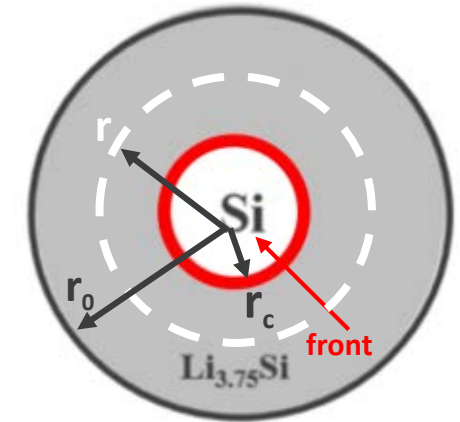
Mechanical problem :

- **1D Mechanical-diffusion problem (spherical geometry):** differential swelling driven by Lithium concentration.
- **Displacement field solution is radial :** $u(r, t) = u(r, t) e_r$
- **Boundaries conditions:** $\sigma_{rr}(r_0, t) = 0$ $u(0, t) = 0$
- **Strain components (compatibility):** $\epsilon_{rr} = \frac{\partial u(r, t)}{\partial r}$ $\epsilon_{\theta\theta} = \epsilon_{\phi\phi} = \frac{u(r, t)}{r}$
- **Equilibrium:** $\frac{\partial \sigma_{rr}}{\partial r} + \frac{2}{r} [\sigma_{rr} - \sigma_{\theta\theta}] = 0$



Mechanical problem :

- **1D Mechanical-diffusion problem (spherical geometry):** differential swelling driven by Lithium concentration.
- **Displacement field solution is radial :** $u(r, t) = u(r, t) e_r$
- **Boundaries conditions:** $\sigma_{rr}(r_0, t) = 0 \quad u(0, t) = 0$
- **Strain components (compatibility):** $\epsilon_{rr} = \frac{\partial u(r, t)}{\partial r} \quad \epsilon_{\theta\theta} = \epsilon_{\phi\phi} = \frac{u(r, t)}{r}$
- **Equilibrium:** $\frac{\partial \sigma_{rr}}{\partial r} + \frac{2}{r} [\sigma_{rr} - \sigma_{\theta\theta}] = 0$



Ingredients for the core/shell mechanical model :

- **Chemical deformation (Zhang et al. 2007) :** $\underline{\underline{\epsilon}}^c(r, t) = \beta \hat{c}(r, t) \underline{\underline{I}}$
- **Elastic properties depend linearly on lithium concentration. Pristine silicon: $E_0 = 160$ GPa, $\nu = 0.25$, Lithiated silicon ($\text{Li}_{3.75}\text{Si}$): $E_S = 40$ GPa, $\nu = 0.22$ (Shenoy et al. 2010).**

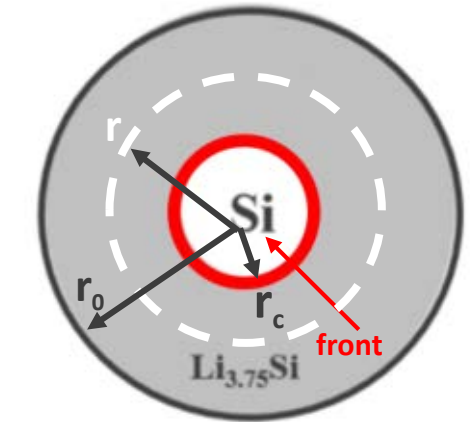
$$\mu(r, t) = \frac{1}{2} \frac{E_0[1 - \hat{c}(r, t)] + E_S \hat{c}(r, t)}{(1 + \nu_0[1 - \hat{c}(r, t)] + \nu_S \hat{c}(r, t))}$$

$$\kappa(r, t) = \frac{1}{3} \frac{E_0[1 - \hat{c}(r, t)] + E_S \hat{c}(r, t)}{1 - 2(\nu_0[1 - \hat{c}(r, t)] + \nu_S \hat{c}(r, t))}$$

Ingredients for the core/shell mechanical model :

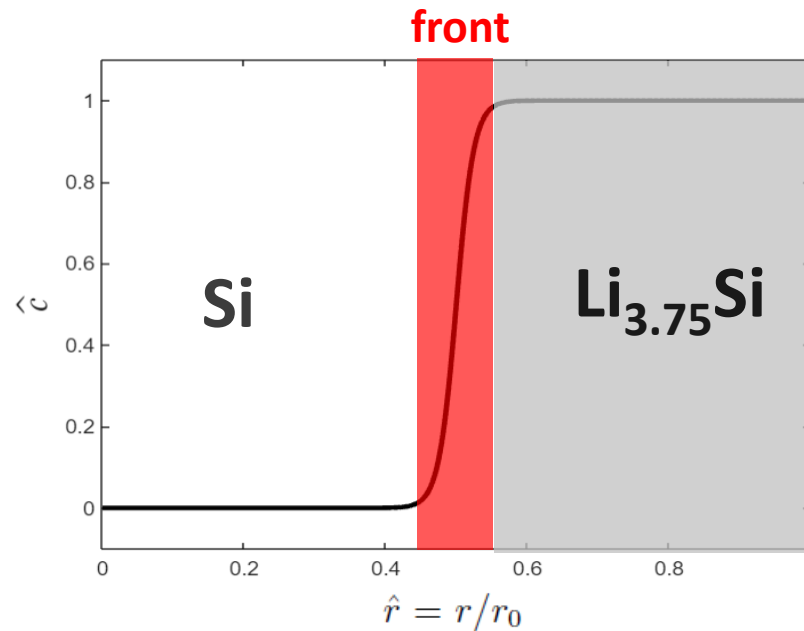
- Inelasticity: viscoplastic deformation using Norton's Law (Huang et al. 2013, Seck et al. 2018)

$$\underline{\dot{\epsilon}}^{vp}(r, t) = 3 \underline{\underline{s}}(r, t) \frac{\partial w}{\partial \tilde{\sigma}}(\tilde{\sigma}) \quad w(\tilde{\sigma}) = \frac{\dot{\epsilon}_0 \sigma_Y}{\frac{1}{m} + 1} \left(\frac{\tilde{\sigma}}{\sigma_Y} \right)^{\frac{1}{m} + 1} \quad \tilde{\sigma} = \sigma_{eq}^2 \quad \sigma_{eq} = \sqrt{3 \underline{\underline{s}} : \underline{\underline{s}} / 2}$$



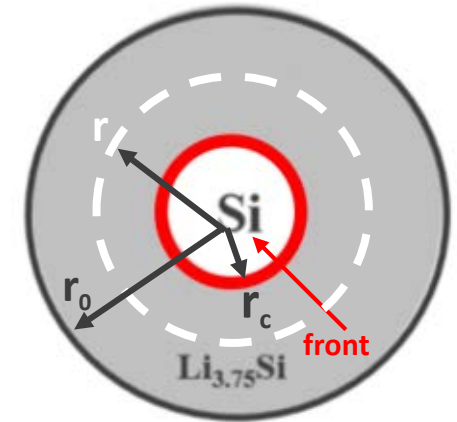
- Lithiation front : logistic function (Huang et al. 2013).

$$\hat{c}(t, r) = \frac{1}{[1 + Qe^{-B(r-r_c(t))}]^{1/\alpha}}$$



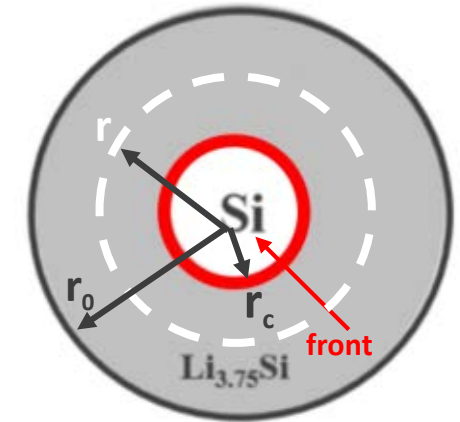
Semi-analytical small strain model

- Extension of the model of (Seck et al. 2018). Main differences :
 - Materials properties dependent on space and time (phase change and lithiation front movement).
 - The interface between the two phases is given as a continuum function (logistic) with a finite thickness.



Semi-analytical small strain model

- Extension of the model of (Seck et al. 2018). Main differences :
 - Materials properties dependent on space and time (phase change and lithiation front movement).
 - The interface between the two phases is given as a continuum function (logistic) with a finite thickness.



Formulation :

- Total strain rate : $\underline{\dot{\underline{\epsilon}}}(r, t) = \underline{\dot{\underline{\epsilon}}}^c(r, t) + \underline{\dot{\underline{\epsilon}}}^e(r, t) + \underline{\dot{\underline{\epsilon}}}^{vp}(r, t)$



- Constitutive law :

$$\underline{\dot{\underline{\epsilon}}}(r, t) = \left(\underbrace{\left[\frac{\dot{\sigma}_m(\mathbf{x}, t)}{3\kappa(r, t)} - \frac{\sigma_m(r, t)\dot{\kappa}(r, t)}{3\kappa^2(r, t)} \right]}_{\text{elastic}} + \underbrace{\left[\dot{\epsilon}^c(r, t) \right]}_{\text{chemical}} \right) \underline{\mathbf{I}} + \underbrace{\left[\frac{\dot{\underline{\mathbf{s}}}(r, t)}{2\mu(r, t)} \right]}_{\text{elastic}} + \underbrace{\left(\left[3 \frac{\partial w}{\partial \tilde{\sigma}}(\tilde{\sigma}) \right] - \underbrace{\left[\frac{\dot{\mu}(r, t)}{2\mu^2(r, t)} \right]}_{\text{elastic}} \right)}_{\text{viscoplastic}} \underline{\mathbf{s}}(r, t) \quad (1)$$

Formulation:

- **Time derivation of compatibility:** $\dot{\epsilon}_{rr}(r, t) - \dot{\epsilon}_{\theta\theta}(r, t) = \frac{r}{3} \frac{\partial}{\partial r} \left(\frac{V_r}{r} \right)$ (2) $V_r(r, t) = \dot{u}(r, t)$
- **Deviatoric part of the constitutive law :** $(\dot{\epsilon}_{rr} - \dot{\epsilon}_{\theta\theta}) \underline{\underline{\mathbf{d}}} = - \left(\frac{\dot{\sigma}_S}{2\mu} - \frac{\sigma_S \dot{\mu}}{2\mu^2} \right) \underline{\underline{\mathbf{d}}} - 3 \sigma_S \frac{\partial w}{\partial \tilde{\sigma}} \underline{\underline{\mathbf{d}}}$ (3) $\underline{\underline{\mathbf{d}}} = \begin{pmatrix} 2 & 0 & 0 \\ 0 & -1 & 0 \\ 0 & 0 & -1 \end{pmatrix}$
 $\sigma_S = \sigma_{\theta\theta} - \sigma_{rr}$
- **Combining (2) and (3) we obtain:** $\dot{\sigma}_S + \sigma_S \left(6\mu(r, t) \frac{\partial w}{\partial \tilde{\sigma}}(r, \tilde{\sigma}) - \frac{\dot{\mu}(r, t)}{\mu(r, t)} \right) = -2\mu(r, t) \left[r \frac{\partial}{\partial r} \left(\frac{V_r}{r} \right) \right]$ (4)

Formulation:

- **Time derivation of compatibility:** $\dot{\epsilon}_{rr}(r, t) - \dot{\epsilon}_{\theta\theta}(r, t) = \frac{r}{3} \frac{\partial}{\partial r} \left(\frac{V_r}{r} \right)$ (2) $V_r(r, t) = \dot{u}(r, t)$
- **Deviatoric part of the constitutive law :** $(\dot{\epsilon}_{rr} - \dot{\epsilon}_{\theta\theta}) \underline{\underline{d}} = - \left(\frac{\dot{\sigma}_S}{2\mu} - \frac{\sigma_S \dot{\mu}}{2\mu^2} \right) \underline{\underline{d}} - 3 \sigma_S \frac{\partial w}{\partial \tilde{\sigma}} \underline{\underline{d}}$ (3) $\underline{\underline{d}} = \begin{pmatrix} 2 & 0 & 0 \\ 0 & -1 & 0 \\ 0 & 0 & -1 \end{pmatrix}$
 $\sigma_S = \sigma_{\theta\theta} - \sigma_{rr}$
- **Combining (2) and (3) we obtain:** $\dot{\sigma}_S + \sigma_S \left(6\mu(r, t) \frac{\partial w}{\partial \tilde{\sigma}}(r, \tilde{\sigma}) - \frac{\dot{\mu}(r, t)}{\mu(r, t)} \right) = -2\mu(r, t) \left[r \frac{\partial}{\partial r} \left(\frac{V_r}{r} \right) \right]$ (4)

Final :

$$\hat{u}(r, t) = \frac{u(r, t)}{r}, \hat{\kappa}(r, t) = \frac{\kappa(r, t)}{\sigma_Y}$$

$$\hat{\mu}(r, t) = \frac{\mu(r, t)}{\sigma_Y}, \hat{\sigma}(r, t) = \frac{\sigma_S(r, t)}{\sigma_Y}$$

$$\hat{F}(r, t) = \int_0^r \hat{\kappa}(x, t) \varepsilon^c(x, t) x^2 dx$$

Final system

$$\frac{1}{\hat{\mu}} \frac{\partial \hat{\sigma}(r, t)}{\partial t} - \frac{\dot{\hat{\mu}}(r, t)}{\hat{\mu}^2(r, t)} \hat{\sigma}(r, t) + 3\dot{\varepsilon}_0 (\hat{\sigma}^2(r, t))^{\frac{1}{m}-1} \hat{\sigma}(r, t) + 2r \frac{\partial}{\partial t} \left(\frac{\partial \hat{u}(r, t)}{\partial r} \right) = 0. \quad (5)$$

$$-\hat{\sigma}(r, t) + \frac{3r}{2} \hat{\kappa}(r, t) \frac{\partial \hat{u}(r, t)}{\partial r} + \frac{9}{2r^3} \int_0^r \frac{\partial \hat{\kappa}(r, t)}{\partial x} (x, t) x^3 \hat{u}(x, t) dx + \frac{27}{2r^3} \hat{F}(r, t) - \frac{9}{2r^2} \frac{\partial \hat{F}(r, t)}{\partial r} = 0. \quad (6)$$

- Using the (6), when $r \rightarrow 0 \rightarrow \sigma_S(0, t) = 0$

- One obtain a system of two nonlinear equations (instead of a single equation as in Seck et al. 2018).

Solutions:**A) uniform elastic properties :**

$$\frac{\dot{\sigma}_S(r, t)}{\sigma_Y} + \frac{\xi}{\tau_Y} \left(\frac{\sigma_S(r, t)}{\sigma_Y} \right)^{\frac{1}{m}} = \frac{-r}{3\eta\sigma_Y} \frac{\partial}{\partial r} \left(\frac{3}{r^3} \int_0^r \dot{\epsilon}^c(x, t) x^2 dx \right) \quad (7)$$

$$\tau_Y = \frac{2\sigma_Y\eta}{\dot{\epsilon}_0} \quad \eta = \frac{3\kappa+4\mu}{18\kappa\mu}$$

The proposed method is more robust than that proposed in Huang et al. 2013 :

- **Single integro-differential equation.**
- **No use of a "shooting" type method used to find the velocity field that respects the boundary condition.**

Solutions:

A) Uniform elastic properties :

$$\frac{\dot{\sigma}_S(r, t)}{\sigma_Y} + \frac{\xi}{\tau_Y} \left(\frac{\sigma_S(r, t)}{\sigma_Y} \right)^{\frac{1}{m}} = \frac{-r}{3\eta\sigma_Y} \frac{\partial}{\partial r} \left(\frac{3}{r^3} \int_0^r \dot{\epsilon}^c(x, t) x^2 dx \right) \quad (7)$$

$$\tau_Y = \frac{2\sigma_Y\eta}{\dot{\epsilon}_0} \quad \eta = \frac{3\kappa+4\mu}{18\kappa\mu}$$

B) Complete problem with variation of elastic properties:

- Application of the finite difference method and backward Euler scheme : Spatial domain discretized in N points ($i = 1, 2 \dots N$) and the time domain in M points ($k = 1, 2 \dots M$)
- Integration computed using the trapezoidal rule.
- We obtain a nonlinear integro-differential system written in the vector form (solved in Matlab) :

$$\hat{\mathbf{u}}^k = [\hat{u}_1^k \dots \hat{u}_N^k]^T$$

$$\hat{\boldsymbol{\sigma}}^k = [\hat{\sigma}_1^k \dots \hat{\sigma}_N^k]^T$$

$$\hat{\boldsymbol{\varphi}}^k = [\hat{\boldsymbol{\sigma}}^k \quad \hat{\mathbf{u}}^k]^T$$

$$\underline{\underline{\mathbf{H}}}^{k+1} \hat{\boldsymbol{\varphi}}^{k+1} + \mathcal{G}(\hat{\boldsymbol{\varphi}}^{k+1}) + \mathcal{J}(\hat{\boldsymbol{\varphi}}^k) = \mathbf{0} \quad (8)$$

Initial condition $\sigma_S(0, t) = 0$
 $u(0, t) = 0$ $\longrightarrow \hat{\boldsymbol{\varphi}}^0 = \mathbf{0}$

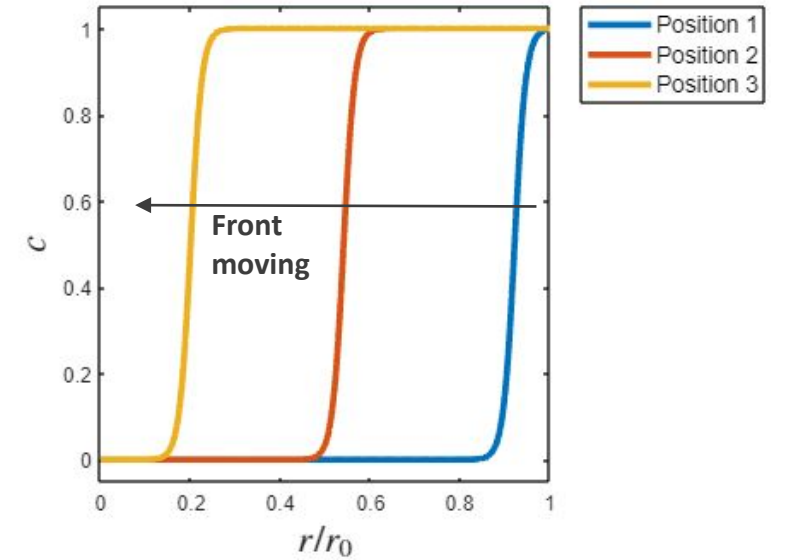
The proposed method is more robust than that proposed in Huang et al. 2013 :

- Single integro-differential equation.
- No use of a "shooting" type method used to find the velocity field that respects the boundary condition.

Geometrical parameters:

- Particle of nanometric size is considered (diameter 20 nm)
- Lithiation front size : 1 nm (Liu et al. 2012)
- Linear evolution of the lithiation front

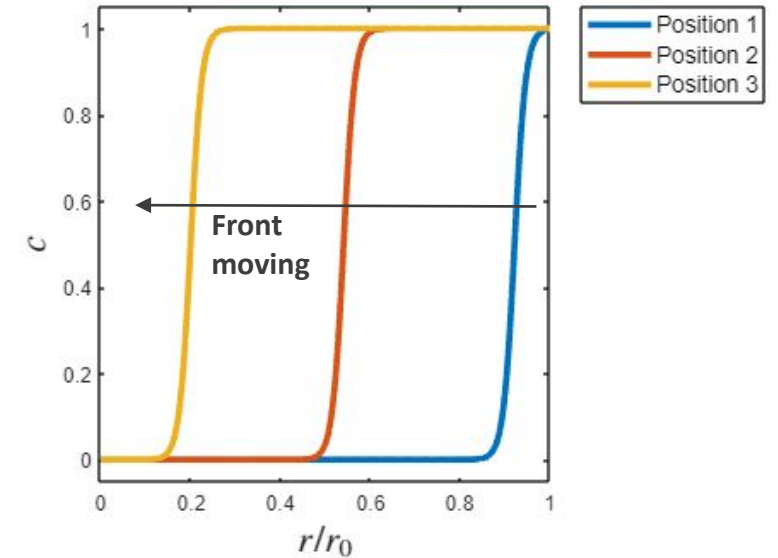
- Lithiation front positions :



Geometrical parameters:

- Particle of nanometric size is considered (diameter 20 nm)
- Lithiation front size : 1 nm (Liu et al. 2012)
- Linear evolution of the lithiation front

• Lithiation front positions :

A - Comparison with Huang et al. 2013 (uniform elastic properties):

Viscoplastic properties (quasi-plastic behaviour)

$$\sigma_Y = 0.05 E_0 \quad m = 0.01 \quad \dot{\epsilon}_0 = 0.001 \text{ s}^{-1}$$

Elastic properties :

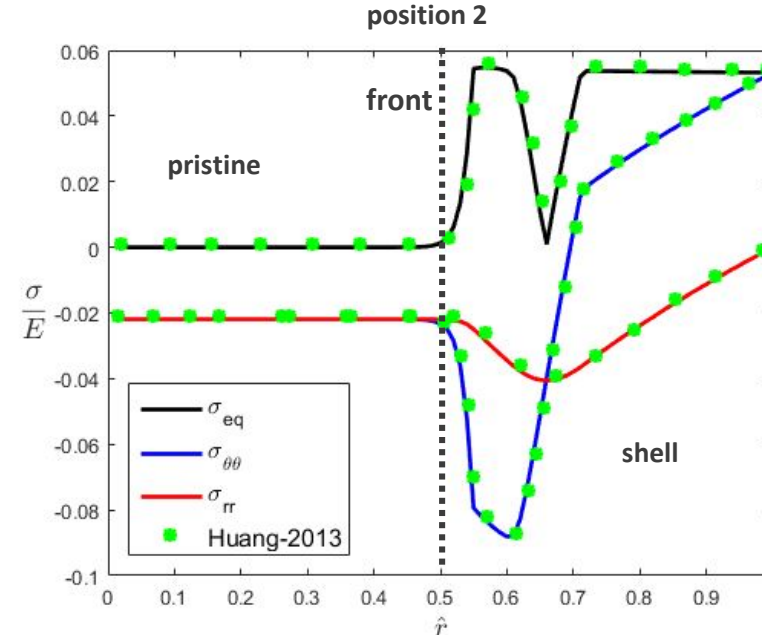
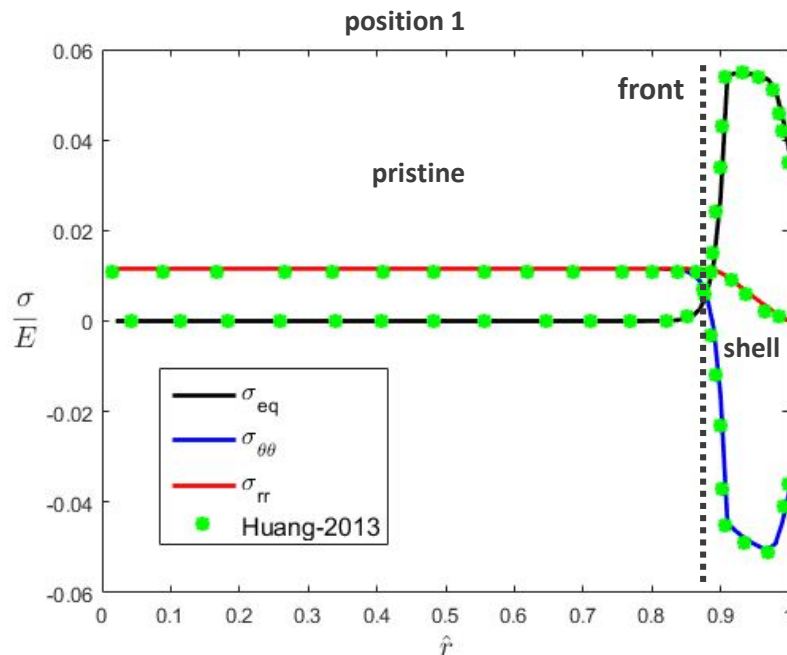
$$E_0 = 160 \text{ GPa} \\ \nu_0 = 0.3$$

Expansion :

$$\beta = 0.26 \\ \text{100\% volume increase}$$

$$N = 300 \\ M = 100$$

Stresses for lithiation front at positions 1 et 2 :



- Results in good agreement with Huang et al. 2013
- Pristine phase in homogeneous hydrostatic state.
- Tension to compression in the pristine.
- Yielding in the shell.

B - More realistic estimation of internal stresses :

Viscoelastic properties (quasi-plastic behaviour)

$$\sigma_Y = 0.05 E_0 \quad m = 0.01 \quad \dot{\epsilon}_0 = 0.001 \text{ s}^{-1}$$

Elastic properties :

$$E_0 = 160 \text{ GPa} \quad \nu_0 = 0.3$$

$$E_c = 0.25 E_0 \quad \nu_c = 0.24$$

Expansion :

$$\beta = 0.6$$

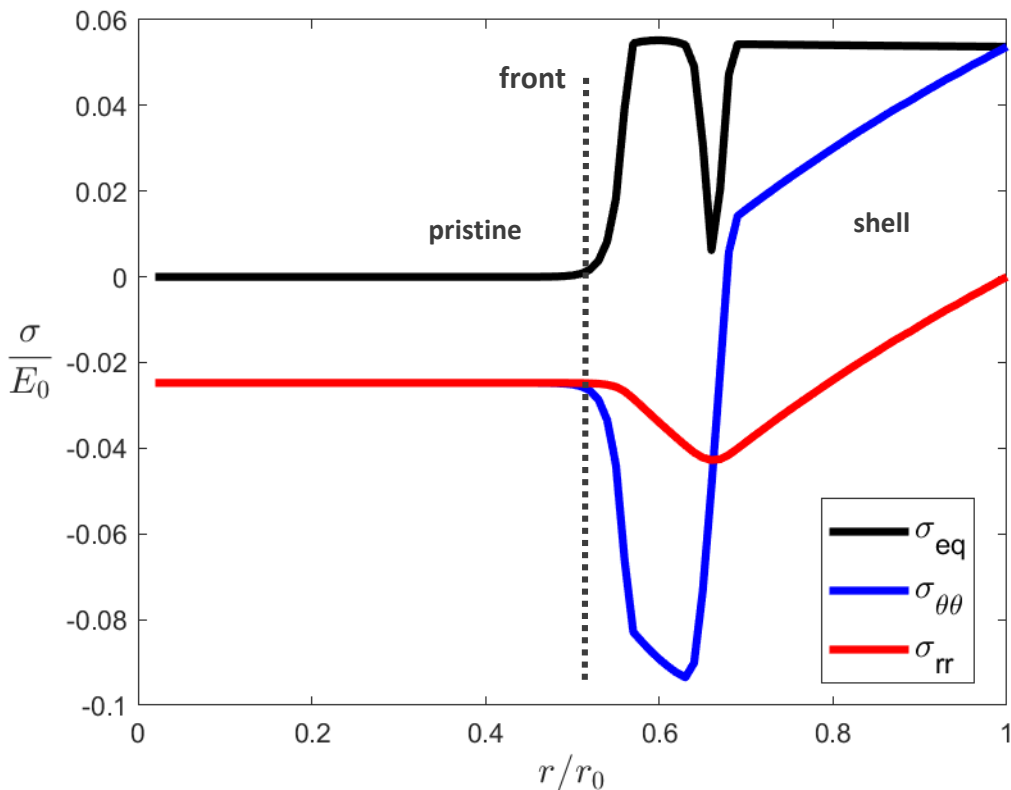
300% volume increase

N = 300

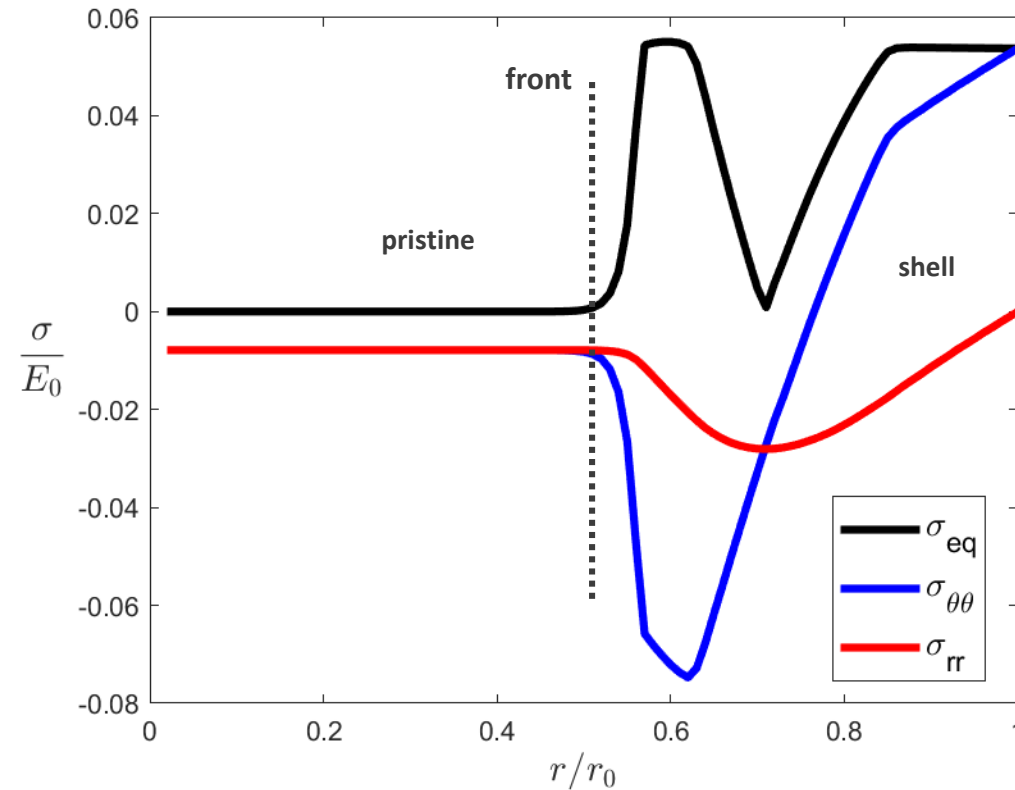
M = 100

Stresses for lithiation front at position 2 :

Stresses with uniform elastic properties



Stresses with variation of elastic properties

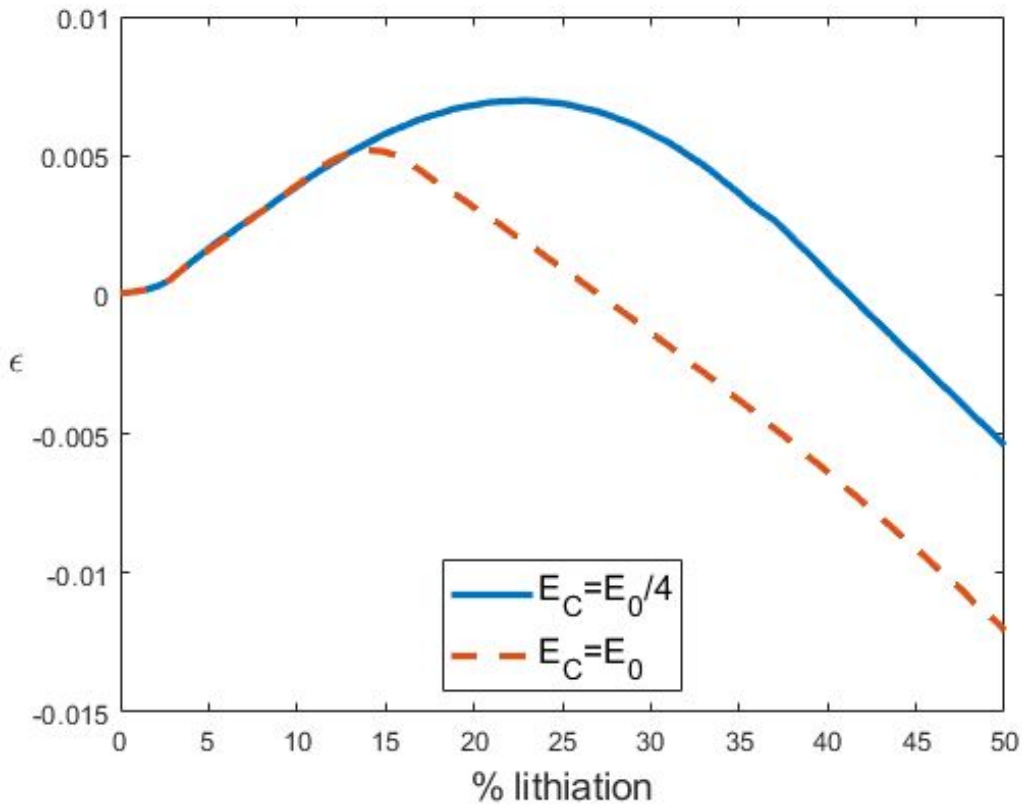


- Decrease of hydrostatic stress in the pristine phase
- Similar stresses in the periphery of the particle

B - More realistic estimation of internal stresses :

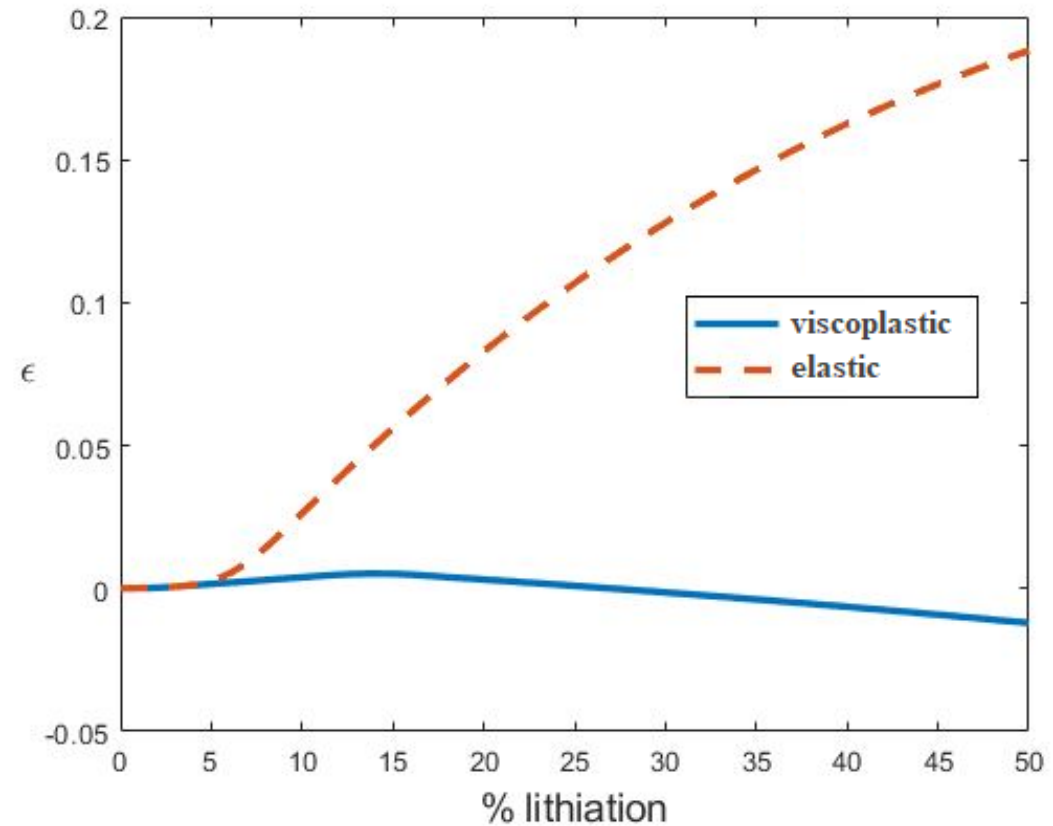
Evolution of hydrostatic strain in the pristine silicon:

With respect to stiffness :



- Overestimation of the strain in the pristine silicon when elastic properties are uniform.

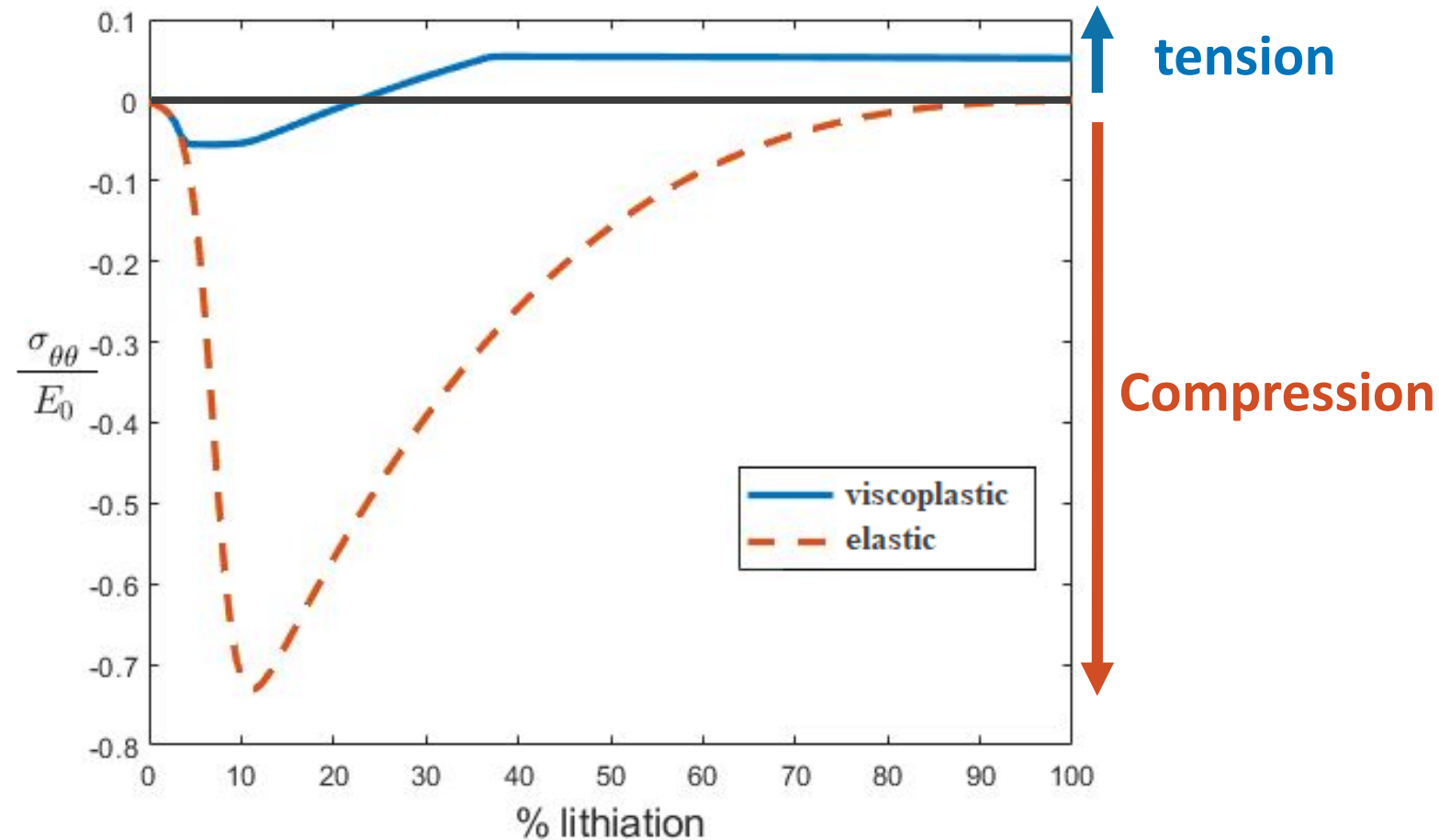
With respect to the material model :



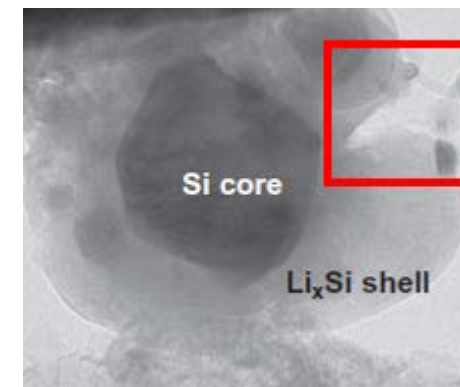
- The strain in the pristine silicon is always positive in the pure elastic model.

C – Pushing out effect :

- Hoop stress at the outer boundary of the particle during lithiation



- Compression to tension behaviour in the viscoplastic model.
- In the elastic case, the hoop stress do not turns in tension.
- Higher stress in the elastic model.
- Stresses are relaxed by plasticity on the lithiation front (Huang et al. 2013).



(S.Huang et al., Acta Materialia 61 (2013))

In this work we proposed :

- An original small strain model of lithiation of a silicon spherical nanoparticle with an advancing lithiation front and phase changing.
- The viscoplastic model is essential to obtain a compression in the pristine silicon and a traction in the lithiated shell.

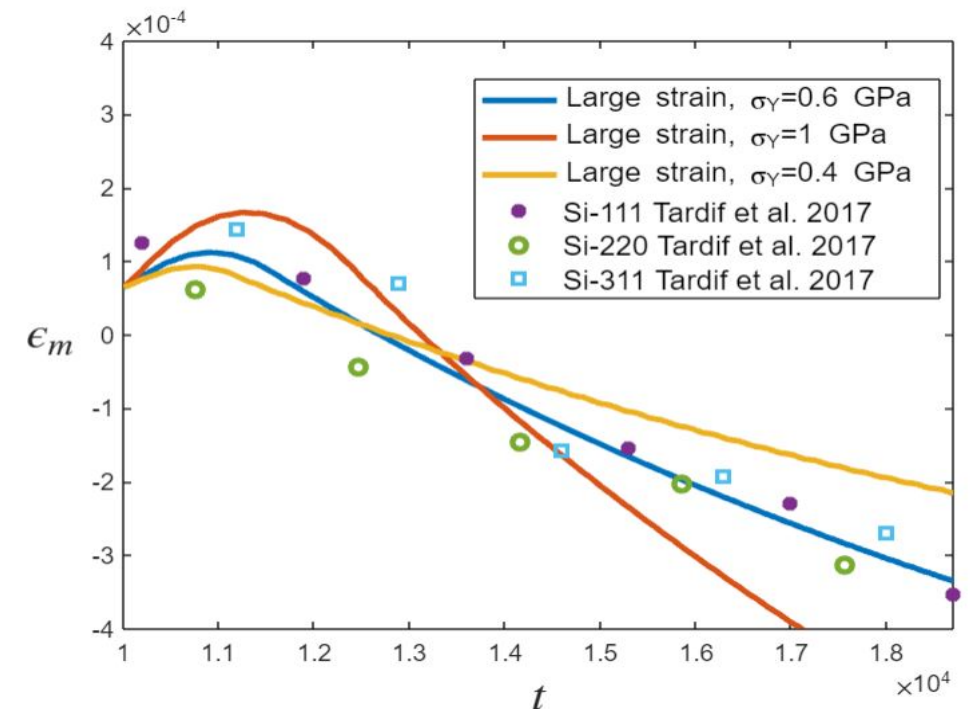
In progress :

- Large strain finite element model
- Comparison with experimental data of the mean strain in the pristine silicon during its first lithiation. (EJM)
- Study of cyclic lithiation/delithiation of silicon particle.
- Study of the effect of a carbon coating.

Perspectives :

Study of an agglomerate of nanoparticles dispersed in a carbon matrix (micrometer size) - a multiscale model:

- Use of mean field and full field methods via FFT calculations.
- Analysis of the carbon matrix/inclusion interaction.



Thank you for your attention!



DE LA RECHERCHE À L'INDUSTRIE



References :

(Huang et al. 2013): Huang, S., Fan, F., Li, J., Zhang, S., and Zhu, T. Stress generation during lithiation of high-capacity electrode particles in lithium ion batteries. *Acta Materialia* 61, 12 (2013), 4354 – 4364.

(Shenoy et al. 2010). Shenoy, V., Johari, P., and Qi, Y. Elastic softening of amorphous and crystalline li-si phases with increasing li concentration: A first-principles study. *Journal of Power Sources* 195, 19 (2010), 6825–6830.

(Zhang et al. 2007) Zhang, X., Shyy, W., and Sastry, A. M. Numerical simulation of intercalation-induced stress in li-ion battery electrode particles. *Journal of the Electrochemical Society* 154, 10 (2007), A910 A916.

(Sethuraman et al. 2010). Sethuraman, V. A., Chon, M. J., Shimshak, M., Srinivasan, V., and Guduru, P. R. In situ measurements of stress evolution in silicon thin films during electrochemical lithiation and delithiation. *Journal of Power Sources* 195, 15 (2010), 5062–5066.

(Seck et al. 2018) Seck, M. E. B., Garajeu, M., and Masson, R. Exact solutions for the effective nonlinear viscoelastic (or elastoviscoplastic) behaviour of particulate composites under isotropic loading. *European Journal of Mechanics-A/Solids* 72 (2018), 223–234.

(Tardif et al. 2017): Tardif, S., Pavlenko, E., Quazuguel, L., Boniface, M., Maréchal, M., Micha, J.-S., Gonon, L., Mareau, V., Gebel, G., Bayle-Guillemaud, P., et al. Operando raman spectroscopy and synchrotron x-ray diffraction of lithiation/delithiation in silicon nanoparticle anodes. *ACS nano* 11, 11 (2017), 11306–11316.

(Sheikholeslami,2018) : Sheikholeslami, Z. S., Yousefi, M., Imani, M., and Joupari, M. D. Low-temperature, chemical vapor deposition of thin-layer pyrolytic carbon coatings derived from camphor as a green precursor. *Journal of Materials Science* 53, 2 (2018), 959–976.

(Li. et al 2016) : Li, W., Cao, K., Wang, H., Liu, J., Zhou, L., and Yao, H. Carbon coating may expedite the fracture of carbon-coated silicon core-shell nanoparticles during lithiation. *Nanoscale* 8, 9 (2016), 5254–5259.

Xiao Hua Liu, Li Zhong, Shan Huang, Scott X Mao, Ting Zhu, and Jian Yu Huang. Sizedependent fracture of silicon nanoparticles during lithiation. *Acs Nano*, 6(2):1522–1531, 2012b.

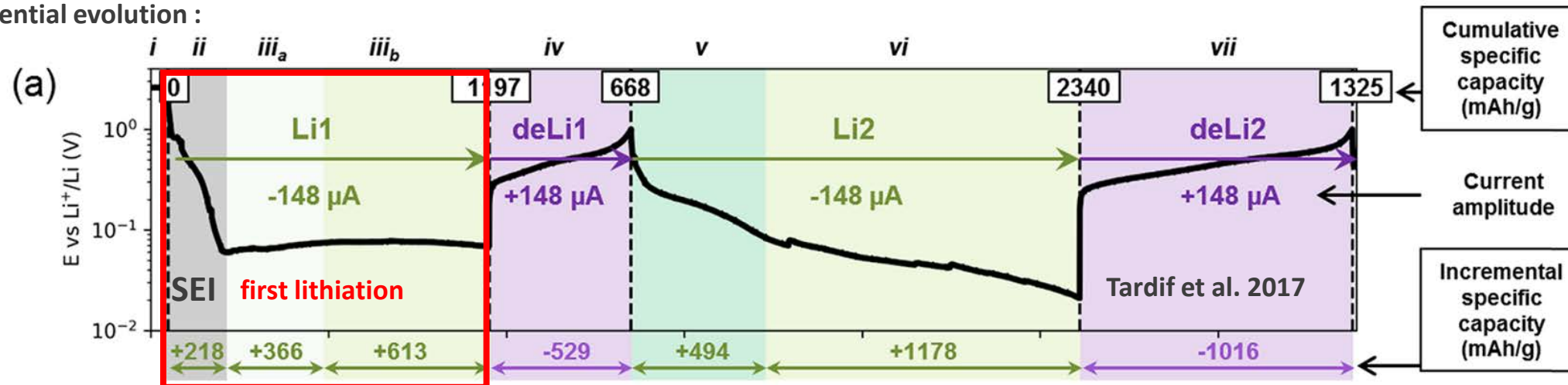
IRESNE | DEC | SESC | LM2C

Institut de recherche sur les systèmes nucléaires pour la production d'énergie bas carbone

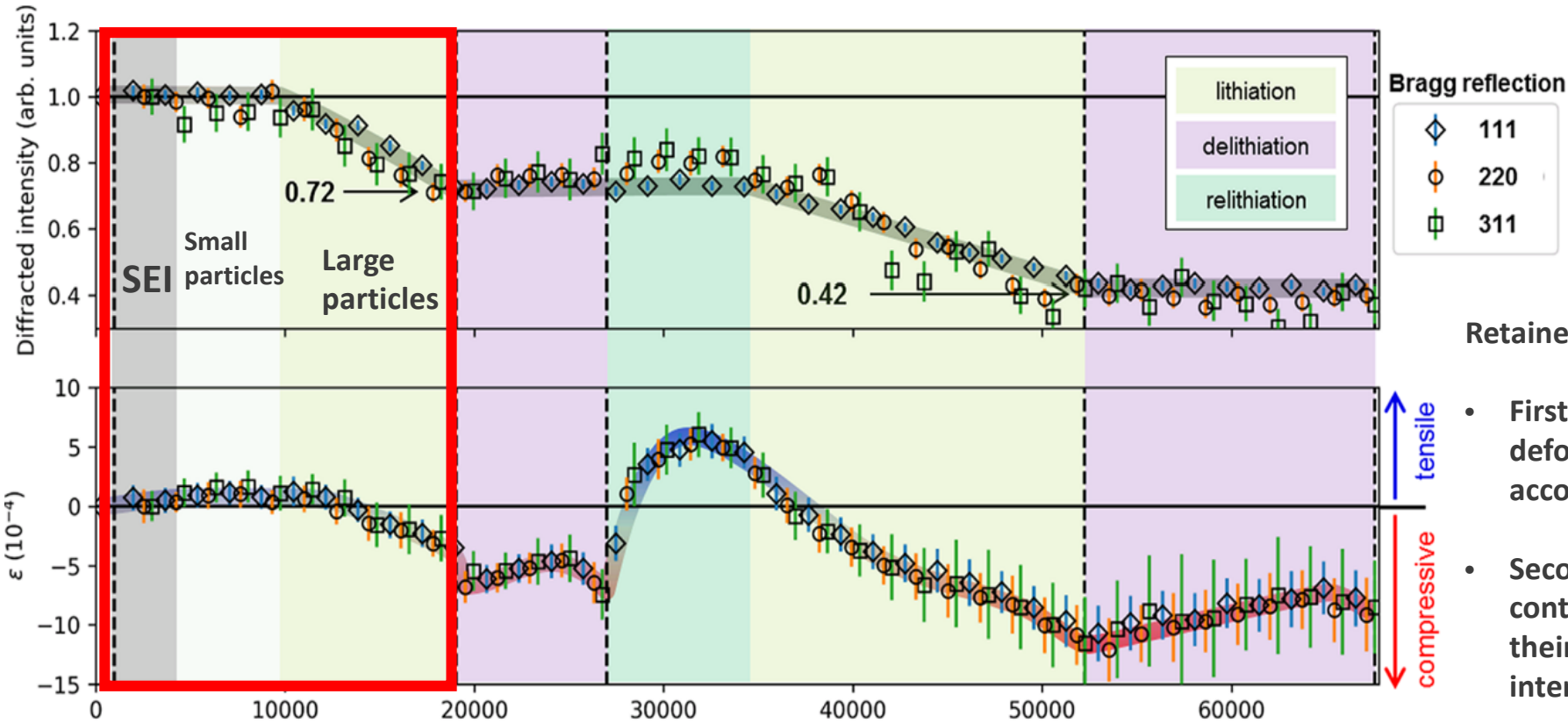
C - Comparison with experimental data (Tardif et al. 2017):

- Experiment technique : X-ray diffraction (XRD) sensitive to the pristine (crystalline part) of the particles.
- Particle system with two populations: large (100 nm) and small (35 nm).
- The particles are in a soft medium.
- Available data:
 - evolution of the specific capacity and potential .
 - evolution of the diffracted intensity of the pristine silicon.
 - average deformation of the pristine.

Potential evolution :



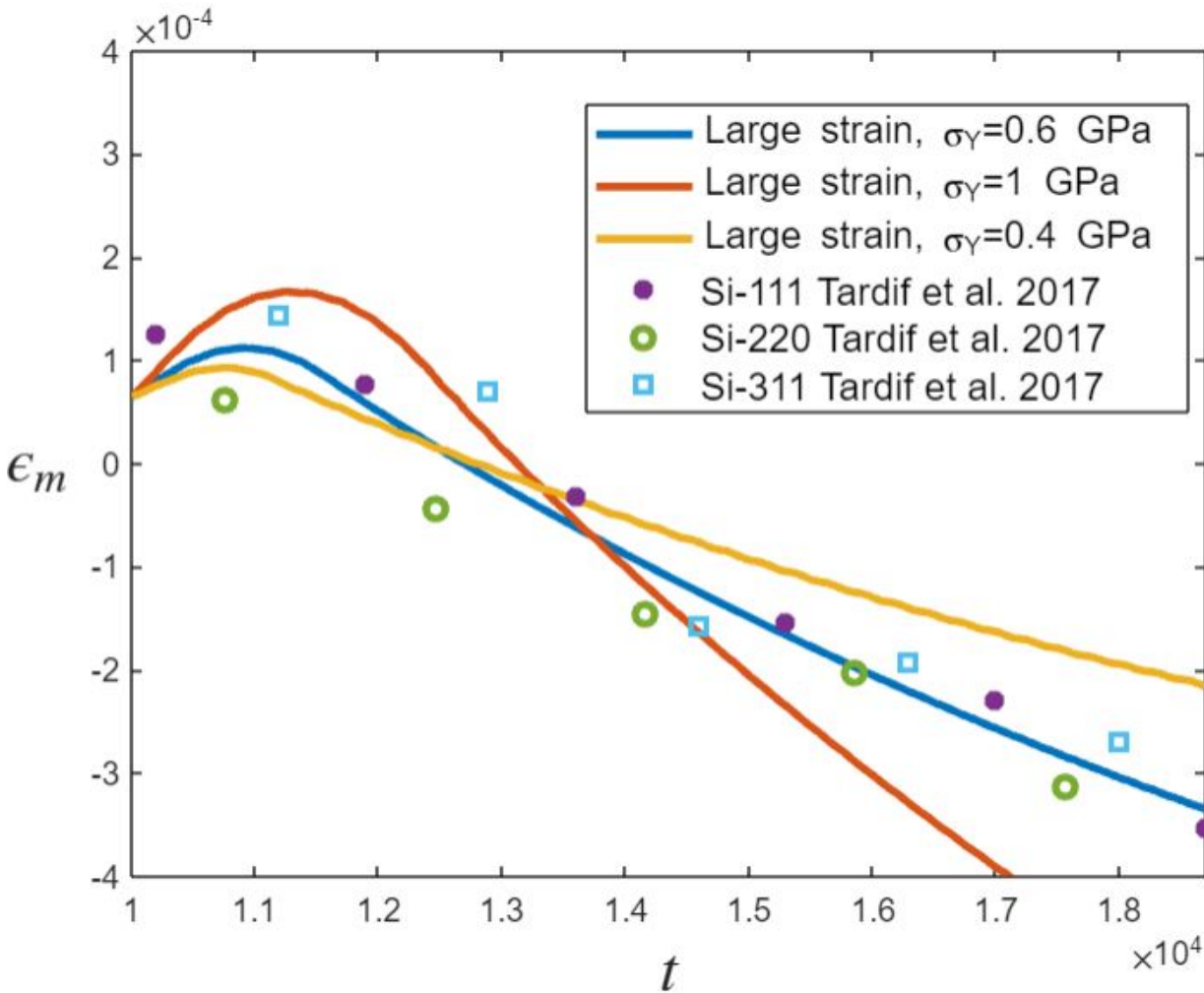
XRD measures during the lithiation of silicon (Tardif et al. 2017) : diffracted intensity (b)



Retained aspects from Tardif et al. 2017 experiment:

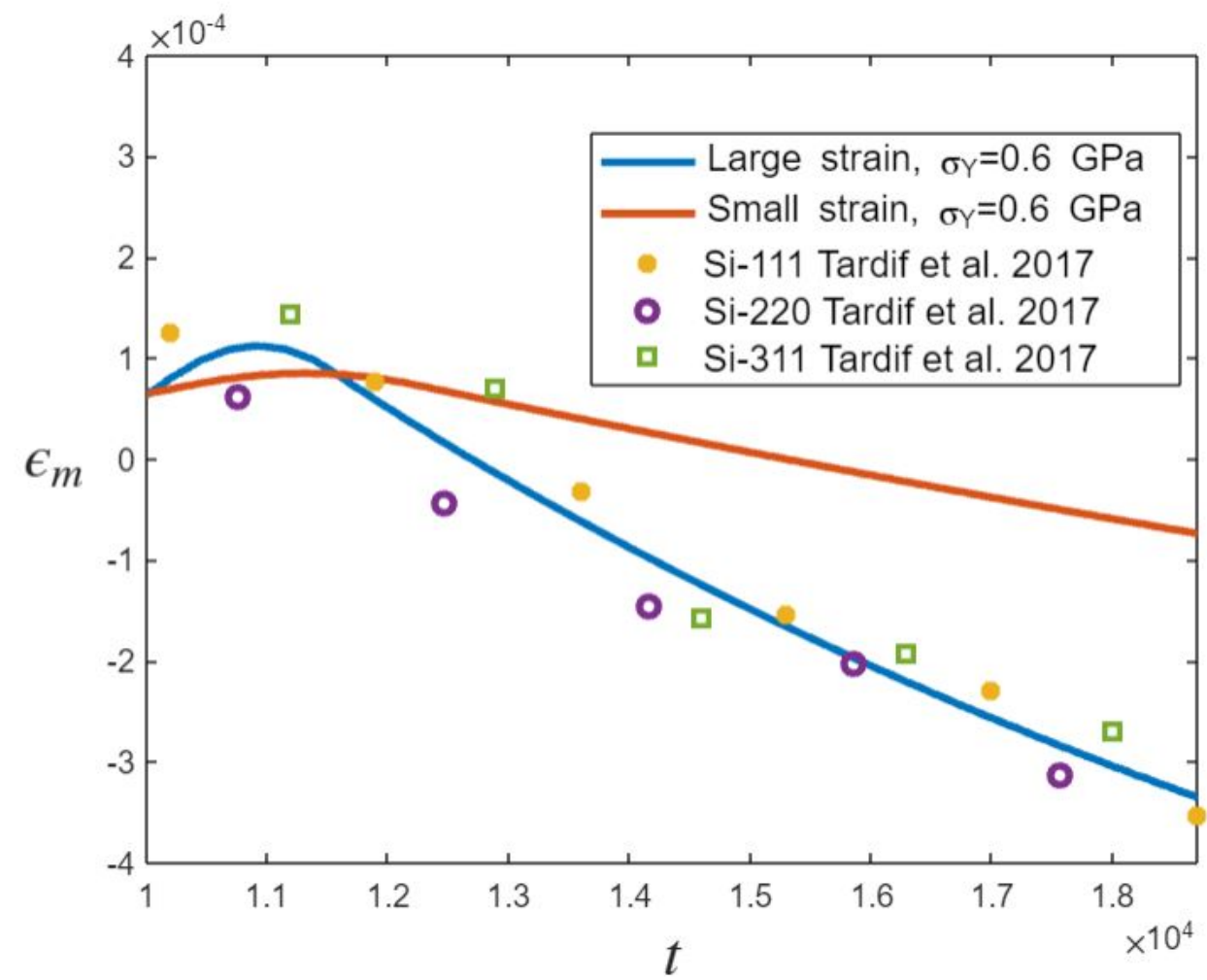
- First part of lithiation : formation of the SEI. The deformation contribution from SEI is taken into account by imposing a radial pressure.
- Second part of lithiation is the small particles: their contribution to the deformation is small because their volume fraction is small (constant diffraction intensity).
- Main contribution to the deformation comes from the large particles (the third part of the lithiation).

Mean strain with respect to the yield stress



Optimal yield stress : 0.6 GPa

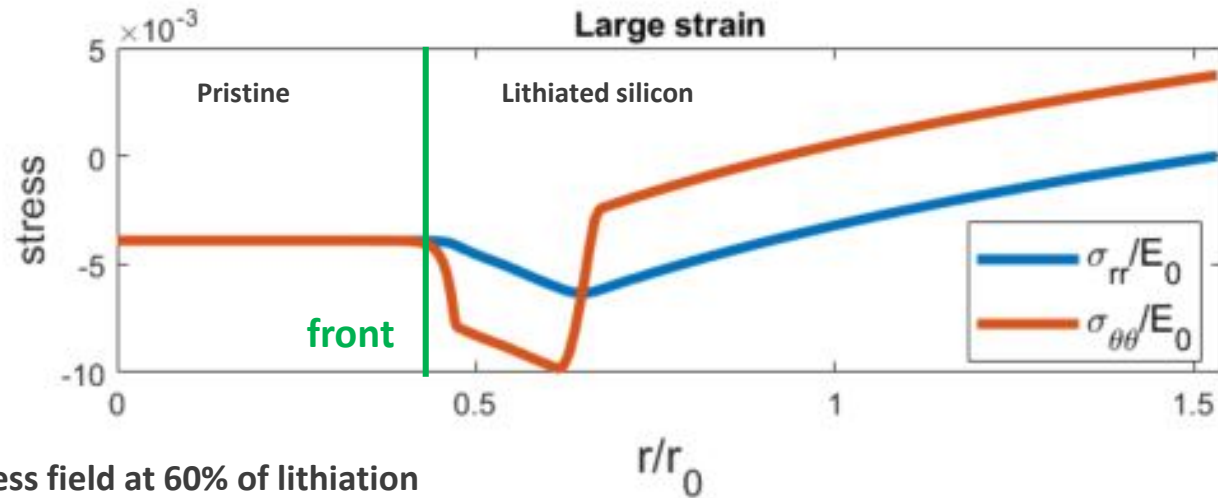
Mean strain comparison : large strain and small strain



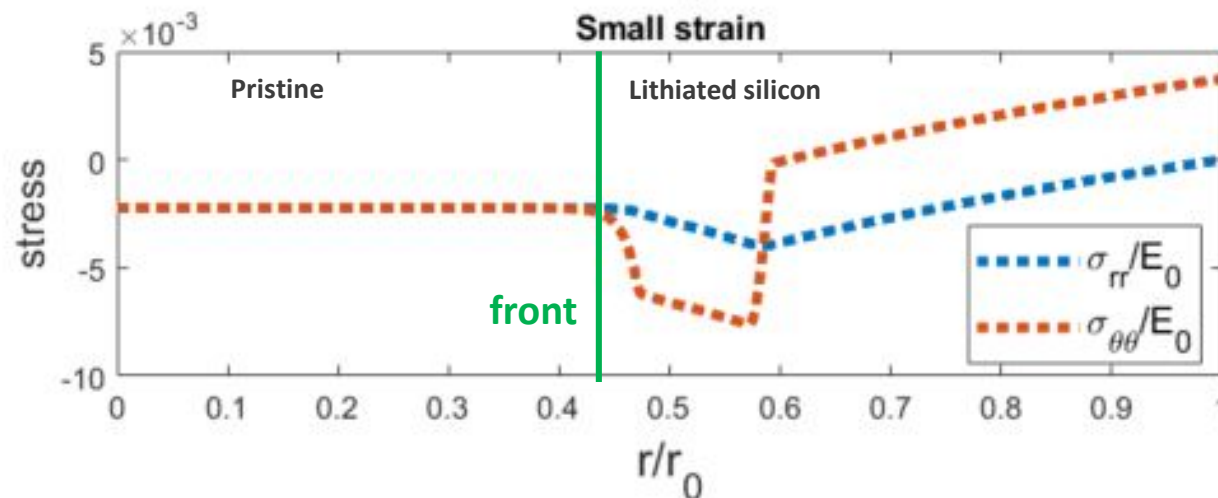
Small strain model overestimates the mean strain in the pristine silicon.

- Large strain is needed because of large volume expansion (300 % expansion) : use of logarithmic strain in the finite element framework (Miehe et al. 2002).

C - Comparison small strain and large strain:



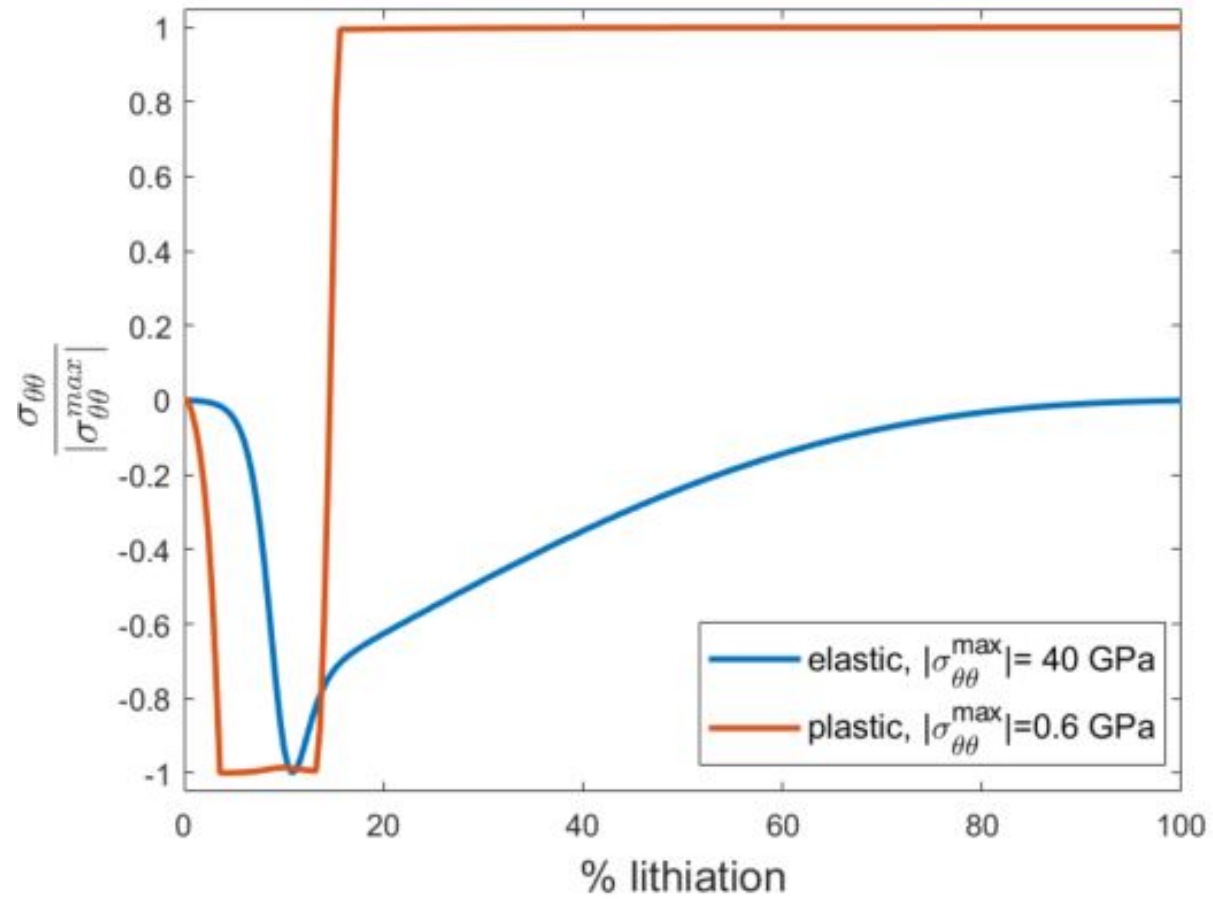
Stress field at 60% of lithiation



Stress analysis :

- Similar stress in the periphery of the particle for both models.
- Hydrostatic stress in the pristine silicon for both models.
- Higher hydrostatic compression in the large strain model (this aspect will be highlighted in the comparison with experiment) and in the interface.

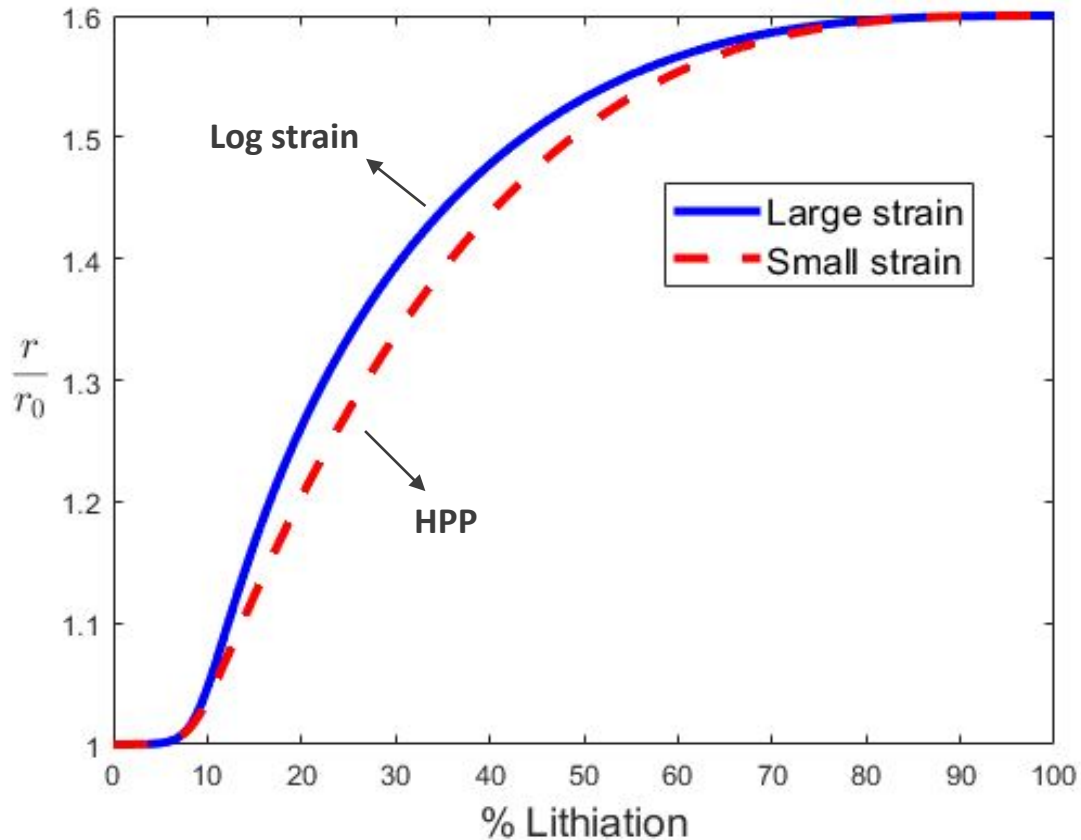
B - Comparison of elastoplastic and elastic models : evolution of hoop stress at the outer border of the particle



- Large strain is needed because of large volume expansion (300 % expansion) : use of logarithmic strain in the finite element framework (Miehe et al. 2002).

B - Comparison small strain and large strain:

- Dimensional evolution :



Dimensional variation:

- Small strain approach underestimates the evolution of the radius.
- Similar evolution between the two approaches at the beginning and at the end of the lithiation.

Interests of using carbon coating :

- Potential buffer effect: limits the volume expansion of silicon.
- Avoids contact between silicon and electrolyte and limits the SEI (solid electrolyte interface).
- Carbon has good conductivity.

Modeling in small strain :

- Linear elastic carbon : solution of an spherical shell submitted to an internal pressure

$$P_c(t) = 3 K_c \left(\frac{u_c(r_0, t)}{r_0} \right) \quad K_c = \kappa_c \left(\frac{(r_{c0}^3 - r_0^3)}{r_0^3 + \left(\frac{3 \kappa_c r_{c0}^3}{4 \mu_c} \right)} \right)$$

interface pressure

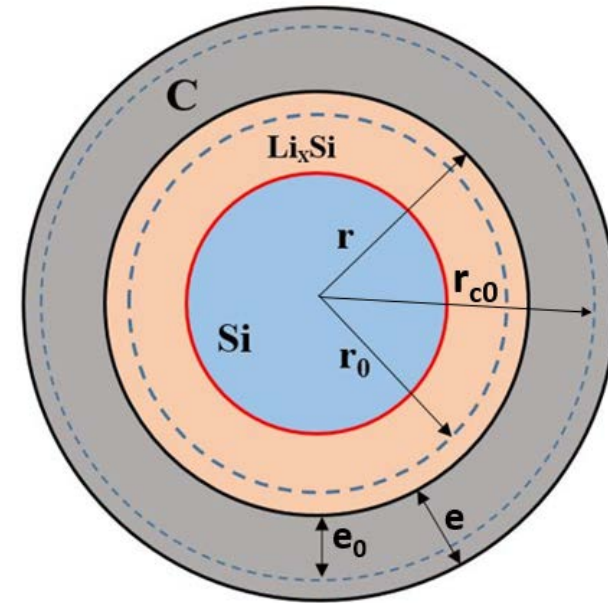
- Displacement field in the carbon coating

$$u_c(r, t) = \frac{P_c(t) r r_0^3}{3 \kappa_c (r_{c0}^3 - r_0^3)} + \frac{P_c(t) r_{c0}^3}{4 \mu_c (r_{c0}^3 - r_0^3)} \left(\frac{r_0^3}{r^2} \right)$$

- Continuity of conditions at the interface : $\sigma_{rr}^c(r_0, t) = \sigma_{rr}(r_0, t) = -P_c(t) \quad u(r_0, t) = u_c(r_0, t)$

- At the end of the lithiation (maximum pressure):
- $$P_c(t_e) = \left(\frac{3 K_c}{1 + \frac{K_c}{\kappa_s}} \right) \varepsilon^c$$

Composite sphere



Carbon stiffness : $E_c = 10$ GPa (pyrolytic carbon)

Geometry update model (at the end of the lithiation) :

- Equations are written in the infinitesimal form, considering the current radius/coating thickness :

$$\delta \hat{r} = \frac{\delta \varepsilon^c \hat{r}}{1 + \frac{\hat{K}_c}{\kappa_s}}$$

$$\delta \hat{e} = \frac{3 \hat{K}_c \delta \varepsilon^c \hat{f}}{1 + \frac{\hat{K}_c}{\kappa_s}}$$

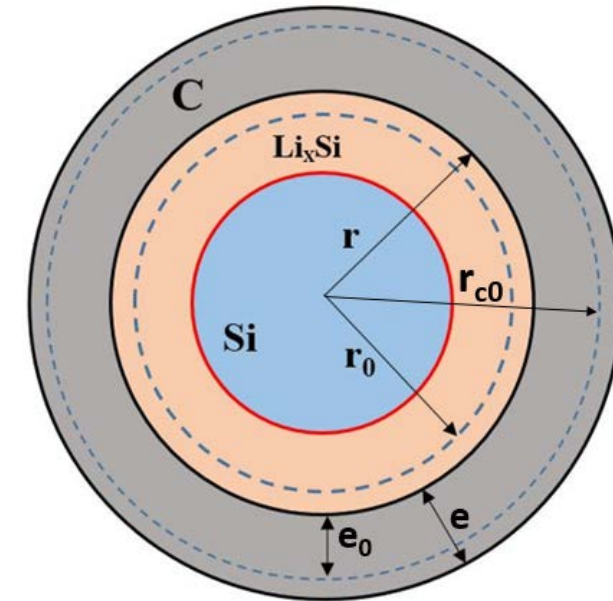
Nonlinear EDO system in function of the normalized current silicon radius and coating thickness

$$\hat{K}_c(e_0/r_0, \hat{r}, \hat{e}) = \kappa_c \frac{\left[\hat{r} + \hat{e} \left(\frac{e_0}{r_0} \right) \right]^3 - \hat{r}^3}{\hat{r}^3 + \frac{3 \kappa_c \left[\hat{r} + \hat{e} \left(\frac{e_0}{r_0} \right) \right]^3}{4 \mu_c}}$$

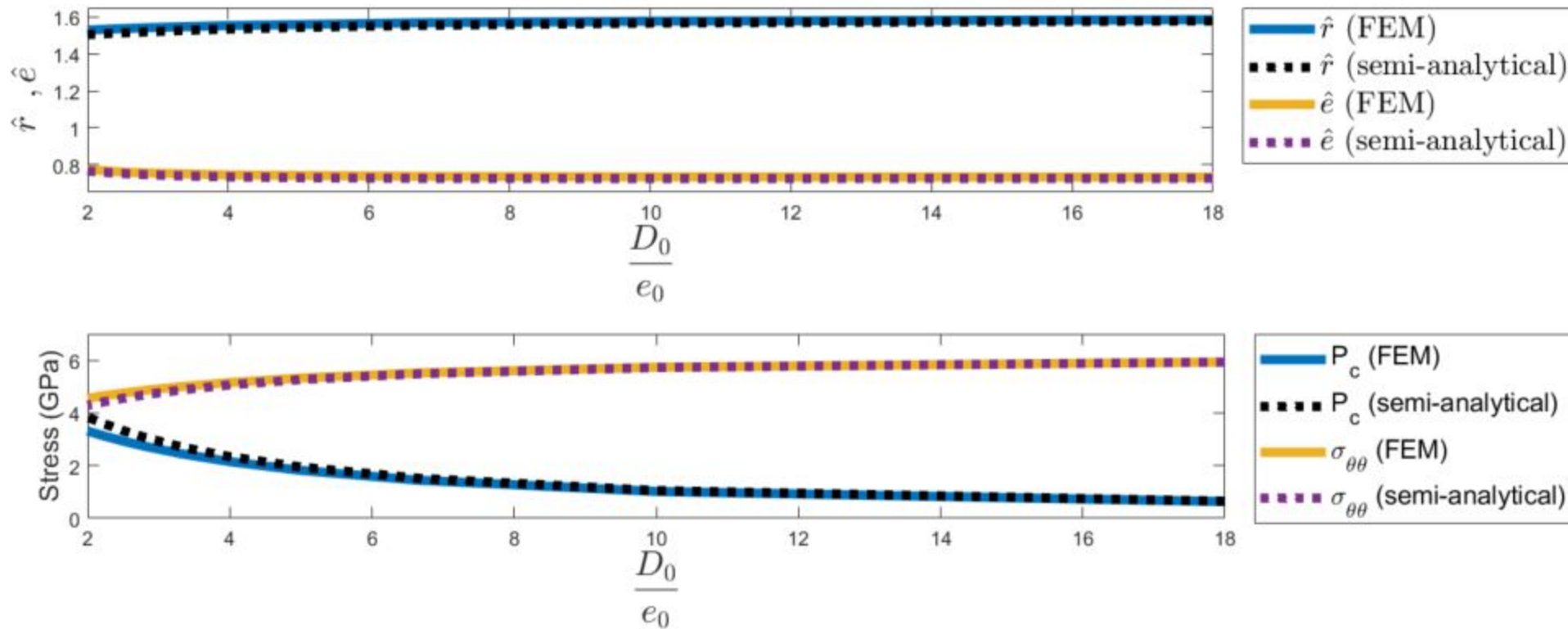
$$\hat{f}(e_0/r_0, \hat{r}, \hat{e}) = \frac{\hat{r}^3 \hat{e} - \left(\left[\hat{r} + \hat{e} \left(\frac{e_0}{r_0} \right) \right]^2 - \hat{r}^2 \right) \left[\hat{e} + \left(\frac{r_0}{e_0} \right) \hat{r} \right] \hat{r}}{\left[\hat{r} + \hat{e} \left(\frac{e_0}{r_0} \right) \right]^3 - \hat{r}^3}$$

Nonlinear geometrical functions

Composite sphere



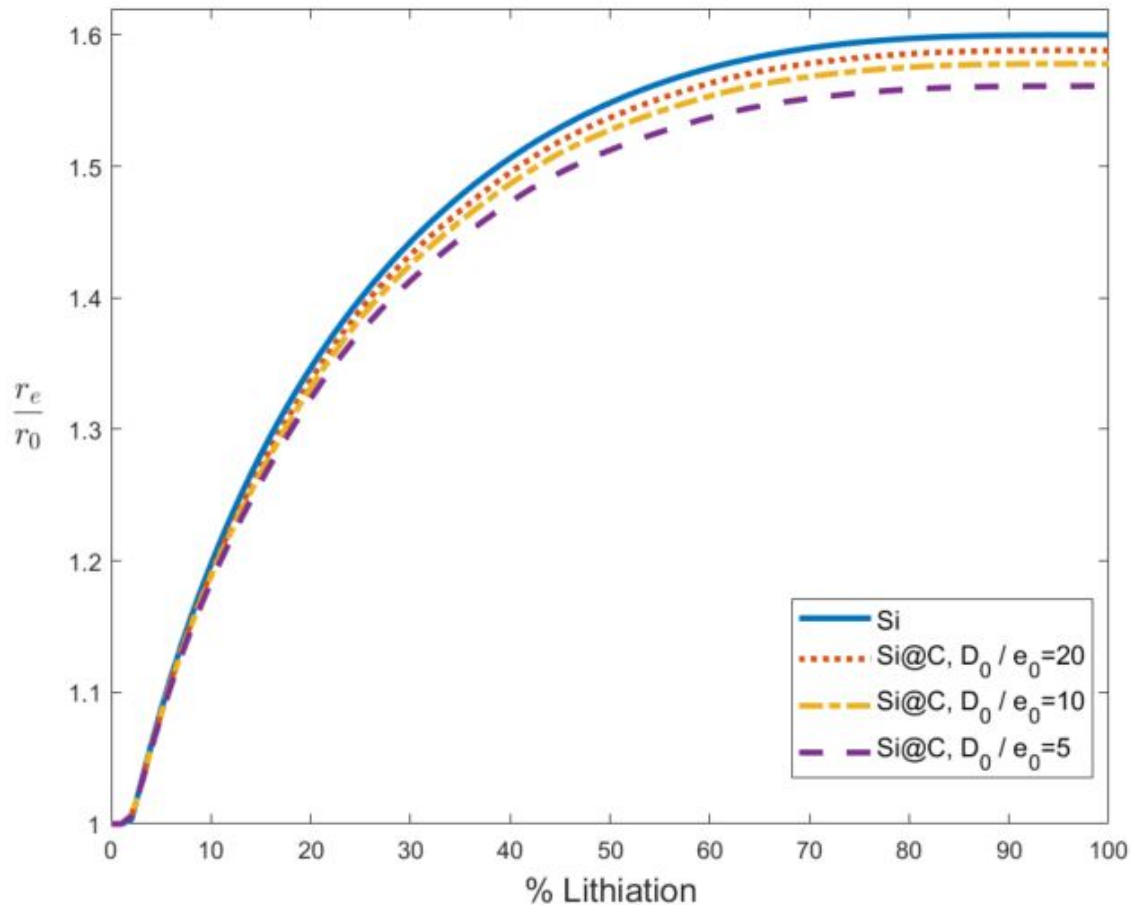
Interface pressure, maximum hoop stress at the carbon coating and dimensional evolution of the silicon and coating at the end of the lithiation (small and geometry update model) :



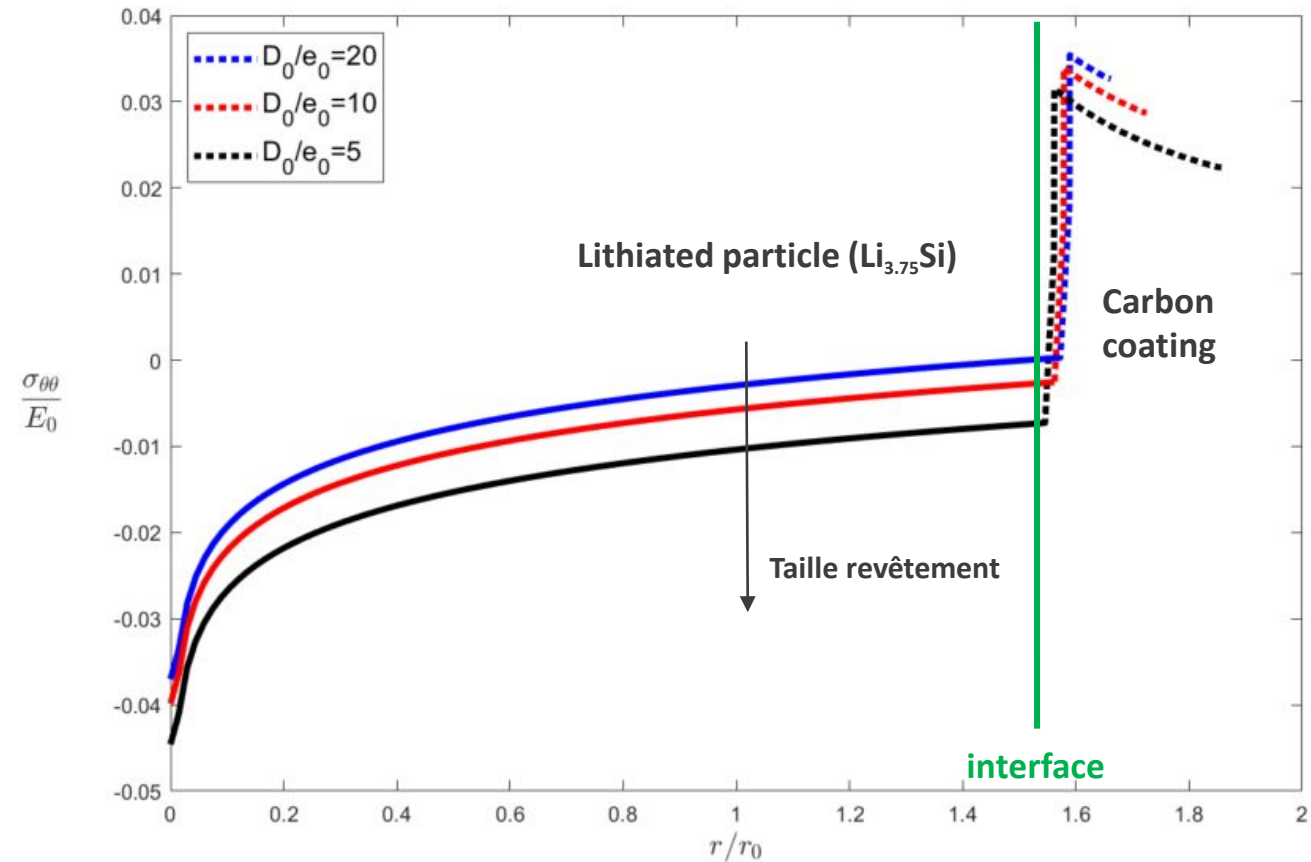
- FEM and semi-analytical solutions in good agreement.
- Slight variation of the maximum hoop stress with respect to particle and carbon coating dimensions.
- Interface pressure increases for a thicker coating.

Modeling II: large strain finite element model

Radius evolution of the silicon



Hoop stress at the end of the lithiation



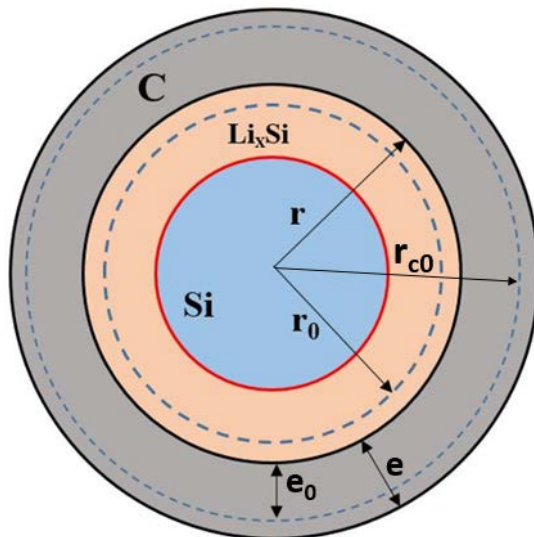
- Slight limitation on volume expansion due to low carbon stiffness.

The particle fully in compression; stress jump at the interface ; carbon in tension

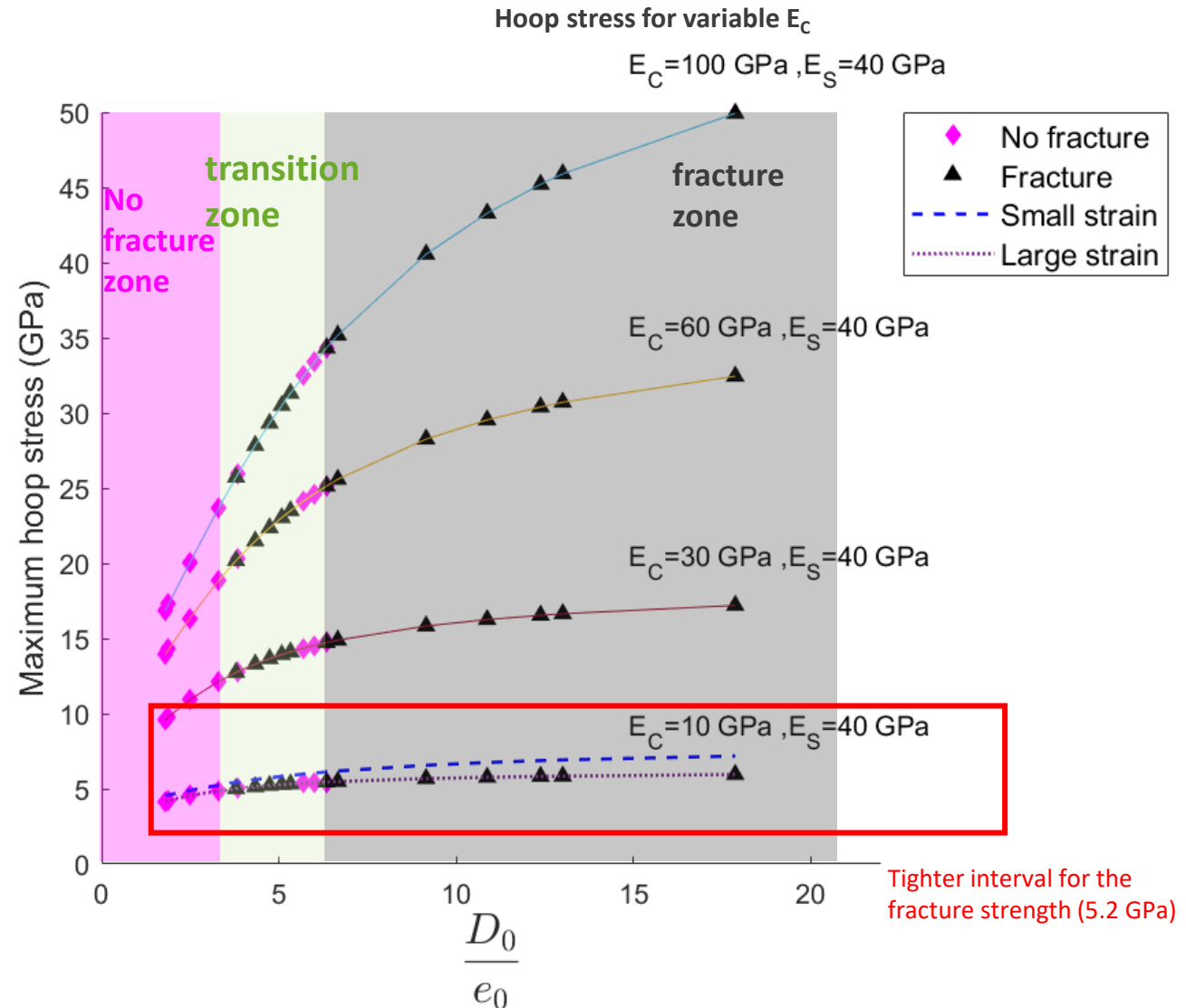
Interests of using carbon coating : Potential buffer effect: limits the volume expansion of silicon ; Avoids contact between silicon and electrolyte and limits the SEI (solid electrolyte interface) ; Carbon has good conductivity.

Semi-analytical solutions at the end of the lithiation :

- Reinterpretation of experimental results of Li et al. 2016 using different properties :
- Li. et al 2016 : $E_C = 300$ GPa and $E_S = 3.5$ GPa for the lithiated silicon (fracture strength between 6 and 12 GPa).
- Literature : $E_S = 40$ GPa and E_C in the order of few dozens of GPa for pyrolytic carbon (Sheikholeslami,2018).



Composite sphere

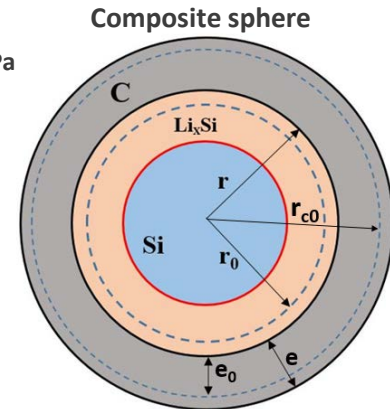


Interests of using carbon coating : Potential buffer effect: limits the volume expansion of silicon ; Avoids contact between silicon and electrolyte and limits the SEI (solid electrolyte interface) ; Carbon has good conductivity.

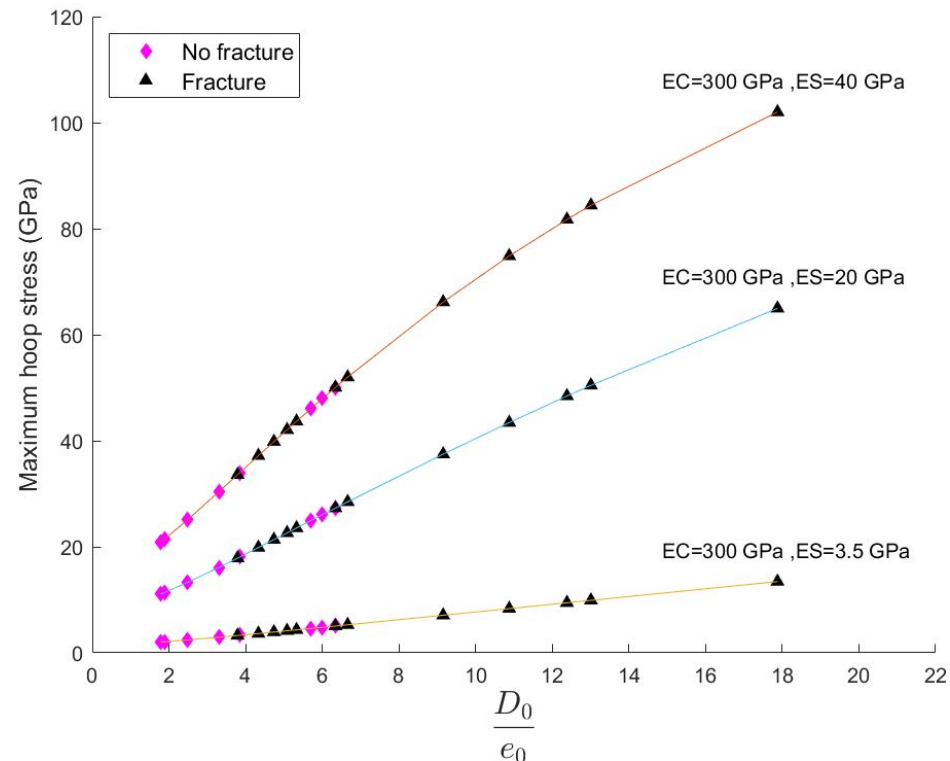
Semi-analytical solutions at the end of the lithiation :

- Reinterpretation of experimental results of Li et al. 2016 using different properties :
- Li. et al 2016 : $E_C = 300$ GPa for the carbon coating and $E_S = 3.5$ GPa for the lithiated silicon (fracture strength between 6 and 12 GPa).
- However according to experiments : $E_S = 40$ GPa and E_C in the order of few dozens of GPa for pyrolytic carbon (Sheikholeslami,2018).

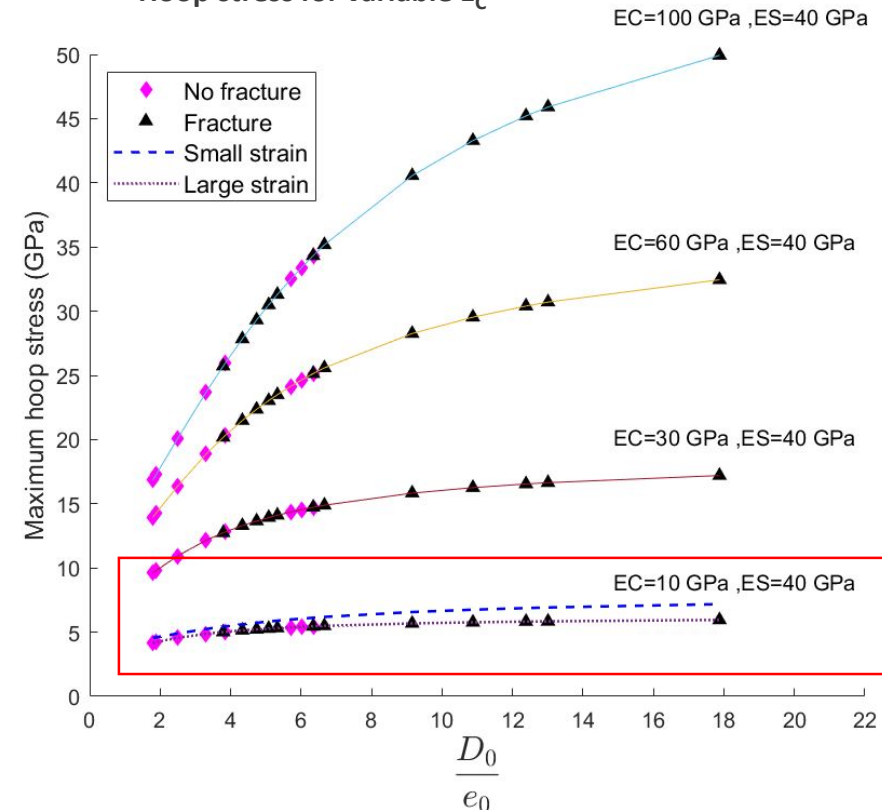
$E_C = 10$ GPa
(pyrolytic
carbon)



Hoop stress for variable E_S



Hoop stress for variable E_C



Extension of the problem of the composite sphere subjected to imposed free deformation (Seck et al. 2018). Materials properties dependent on space and time :

Constitutive equation :

$$\underline{\underline{\dot{\varepsilon}}}(\mathbf{x}, t) = \underbrace{\left(\frac{\dot{\sigma}_m(\mathbf{x}, t)}{3\kappa(\mathbf{x}, t)} - \frac{\sigma_m(\mathbf{x}, t)\dot{\kappa}}{3\kappa^2(\mathbf{x}, t)} \right) \mathbf{I} + \left(\frac{\underline{\underline{\mathbf{s}}}(\mathbf{x}, t)}{2\mu(\mathbf{x}, t)} - \frac{\underline{\underline{\mathbf{s}}}(\mathbf{x}, t)\dot{\mu}(\mathbf{x}, t)}{2\mu^2(\mathbf{x}, t)} \right)}_{\text{elastic}} + \underbrace{3\underline{\underline{\mathbf{s}}}(\mathbf{x}, t) \frac{\partial w}{\partial \tilde{\sigma}}(\tilde{\sigma})}_{\text{viscoplastic}} + \underbrace{\dot{\varepsilon}^c(\mathbf{x}, t) \mathbf{I}}_{\text{chemical}}$$

$$\mu(\mathbf{x}, t) = \frac{1}{2} \frac{E_0[1 - \hat{c}(\mathbf{x}, t)] + E_S \hat{c}(\mathbf{x}, t)}{(1 + \nu_0[1 - \hat{c}(\mathbf{x}, t)] + \nu_S \hat{c}(\mathbf{x}, t))}$$

$$\kappa(\mathbf{x}, t) = \frac{1}{3} \frac{E_0[1 - \hat{c}(\mathbf{x}, t)] + E_S \hat{c}(\mathbf{x}, t)}{1 - 2(\nu_0[1 - \hat{c}(\mathbf{x}, t)] + \nu_S \hat{c}(\mathbf{x}, t))}$$

$$w(\tilde{\sigma}) = \frac{\dot{\varepsilon}_0 \sigma_Y}{\frac{1}{m} + 1} \left(\frac{\tilde{\sigma}}{\sigma_Y} \right)^{\frac{1}{m} + 1} \quad \tilde{\sigma} = \sigma_{eq}^2$$

- Nonlinear system with two variables (normalized displacement and equivalent stress)

Variables:

$$\hat{u}(r, t) = \frac{u(r, t)}{r}, \quad \hat{\kappa}(r, t) = \frac{\kappa(r, t)}{\sigma_Y}$$

$$\hat{\mu}(r, t) = \frac{\mu(r, t)}{\sigma_Y}, \quad \hat{\sigma}(r, t) = \frac{\sigma_S(r, t)}{\sigma_Y}$$

$$\hat{F}(r, t) = \int_0^r \hat{\kappa}(x, t) \varepsilon^c(x, t) x^2 dx$$

$$\frac{1}{\hat{\mu}} \frac{\partial \hat{\sigma}(r, t)}{\partial t} - \frac{\dot{\hat{\mu}}(r, t)}{\hat{\mu}^2(r, t)} \hat{\sigma}(r, t) + 3\dot{\varepsilon}_0 (\hat{\sigma}^2(r, t))^{\frac{1}{m}-1} \hat{\sigma}(r, t) + 2r \frac{\partial}{\partial t} \left(\frac{\partial \hat{u}(r, t)}{\partial r} \right) = 0.$$

$$-\hat{\sigma}(r, t) + \frac{3r}{2} \hat{\kappa}(r, t) \frac{\partial \hat{u}(r, t)}{\partial r} + \frac{9}{2r^3} \int_0^r \frac{\partial \hat{\kappa}(r, t)}{\partial x} (x, t) x^3 \hat{u}(x, t) dx + \frac{27}{2r^3} \hat{F}(r, t) - \frac{9}{2r^2} \frac{\partial \hat{F}(r, t)}{\partial r} = 0.$$

- Combining (5), (8), (9) and integrating by parts we obtain the equation:

$$\sigma_{rr}(r, t) = 3\kappa(r, t) \frac{u(r, t)}{r} - \frac{3}{r^3} \int_0^r \frac{\partial}{\partial x} [\kappa(x, t)] x^2 u(x, t) dx - \frac{9}{r^3} \int_0^r \kappa(x, t) \varepsilon^c(x, t) x^2 dx \quad (10)$$

- From the equilibrium equation:

$$\sigma_S(r, t) = \frac{r}{2} \frac{\partial}{\partial r} [\sigma_{rr}(r, t)] \quad (11)$$

- The second equation of the system is obtained injecting (10) in (11): the unknowns of the nonlinear system are the displacement and the signed stress.

- Using the following normalized variables in (4), (10) and (11), we obtain the final nonlinear integro-differential system. The unknowns are $\hat{u}(r, t)$ and $\hat{\sigma}(r, t)$.

$$\hat{u}(r, t) = \frac{u(r, t)}{r}, \quad \hat{\kappa}(r, t) = \frac{\kappa(r, t)}{\sigma_Y}$$

$$\hat{\mu}(r, t) = \frac{\mu(r, t)}{\sigma_Y}, \quad \hat{\sigma}(r, t) = \frac{\sigma_S(r, t)}{\sigma_Y}$$

→

$$\hat{F}(r, t) = \int_0^r \hat{\kappa}(x, t) \varepsilon^c(x, t) x^2 dx$$

$$\frac{1}{\hat{\mu}} \frac{\partial \hat{\sigma}(r, t)}{\partial t} - \frac{\hat{\mu}(r, t)}{\hat{\mu}^2(r, t)} \hat{\sigma}(r, t) + 3\dot{\varepsilon}_0 (\hat{\sigma}^2(r, t))^{\frac{1}{m}-1} \hat{\sigma}(r, t) + 2r \frac{\partial}{\partial t} \left(\frac{\partial \hat{u}(r, t)}{\partial r} \right) = 0. \quad (12)$$

$$-\hat{\sigma}(r, t) + \frac{3r}{2} \hat{\kappa}(r, t) \frac{\partial \hat{u}(r, t)}{\partial r} + \frac{9}{2r^3} \int_0^r \frac{\partial \hat{\kappa}(r, t)}{\partial x} (x, t) x^3 \hat{u}(x, t) dx + \frac{27}{2r^3} \hat{F}(r, t) - \frac{9}{2r^2} \frac{\partial \hat{F}(r, t)}{\partial r} = 0. \quad (13)$$

- Using the (13), when $r \rightarrow 0 \rightarrow \sigma_S(0, t) = 0$

- Combining (5), (8), (9) and integrating by parts we obtain the equation:

$$\sigma_{rr}(r, t) = 3\kappa(r, t) \frac{u(r, t)}{r} - \frac{3}{r^3} \int_0^r \frac{\partial}{\partial x} [\kappa(x, t)] x^2 u(x, t) dx - \frac{9}{r^3} \int_0^r \kappa(x, t) \varepsilon^c(x, t) x^2 dx \quad (10)$$

- From the equilibrium equation:

$$\sigma_S(r, t) = \frac{r}{2} \frac{\partial}{\partial r} [\sigma_{rr}(r, t)] \quad (11)$$

- The second equation of the system is obtained injecting (10) in (11): the unknowns of the nonlinear system are the displacement and the signed stress.

- Using the following normalized variables in (4), (10) and (11), we obtain the final nonlinear integro-differential system. The unknowns are $\hat{u}(r, t)$ and $\hat{\sigma}(r, t)$

$$\hat{u}(r, t) = \frac{u(r, t)}{r}, \quad \hat{\kappa}(r, t) = \frac{\kappa(r, t)}{\sigma_Y}$$

$$\hat{\mu}(r, t) = \frac{\mu(r, t)}{\sigma_Y}, \quad \hat{\sigma}(r, t) = \frac{\sigma_S(r, t)}{\sigma_Y}$$

$$\hat{F}(r, t) = \int_0^r \hat{\kappa}(x, t) \varepsilon^c(x, t) x^2 dx$$

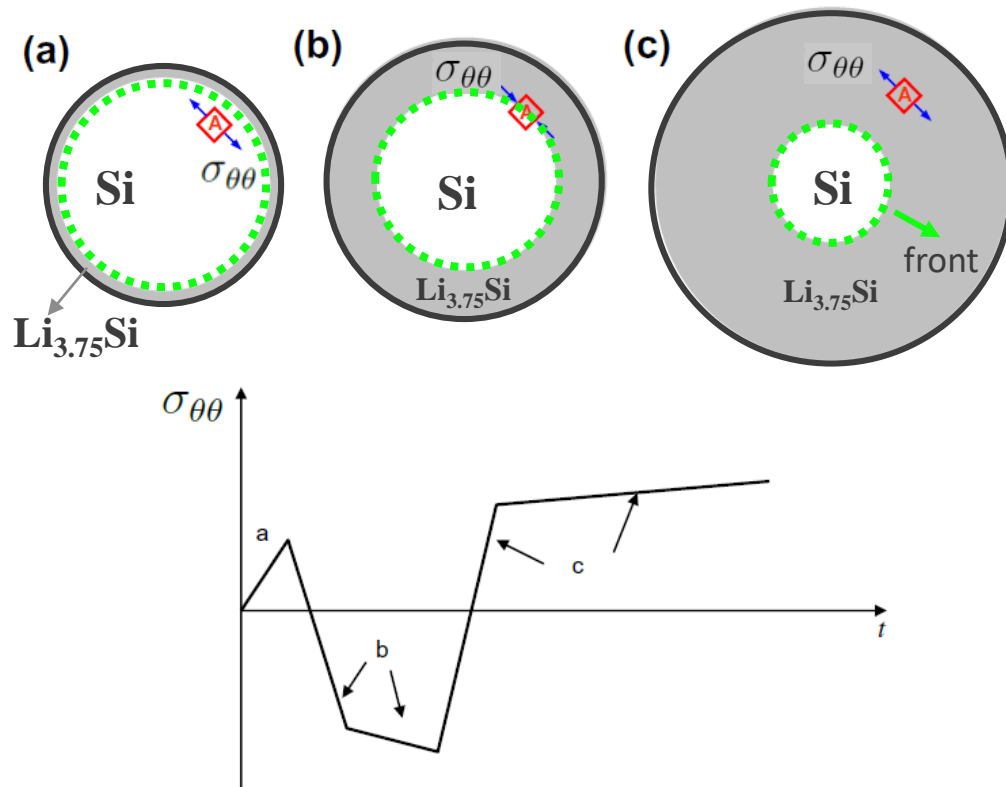
$$\frac{1}{\hat{\mu}} \frac{\partial \hat{\sigma}(r, t)}{\partial t} - \frac{\hat{\mu}(r, t)}{\hat{\mu}^2(r, t)} \hat{\sigma}(r, t) + 3\hat{\varepsilon}_0 (\hat{\sigma}^2(r, t))^{\frac{1}{m}-1} \hat{\sigma}(r, t) + 2r \frac{\partial}{\partial t} \left(\frac{\partial \hat{u}(r, t)}{\partial r} \right) = 0. \quad (12)$$

$$-\hat{\sigma}(r, t) + \frac{3r}{2} \hat{\kappa}(r, t) \frac{\partial \hat{u}(r, t)}{\partial r} + \frac{9}{2r^3} \int_0^r \frac{\partial \hat{\kappa}(r, t)}{\partial x} (x, t) x^3 \hat{u}(x, t) dx + \frac{27}{2r^3} \hat{F}(r, t) - \frac{9}{2r^2} \frac{\partial \hat{F}(r, t)}{\partial r} = 0. \quad (13)$$

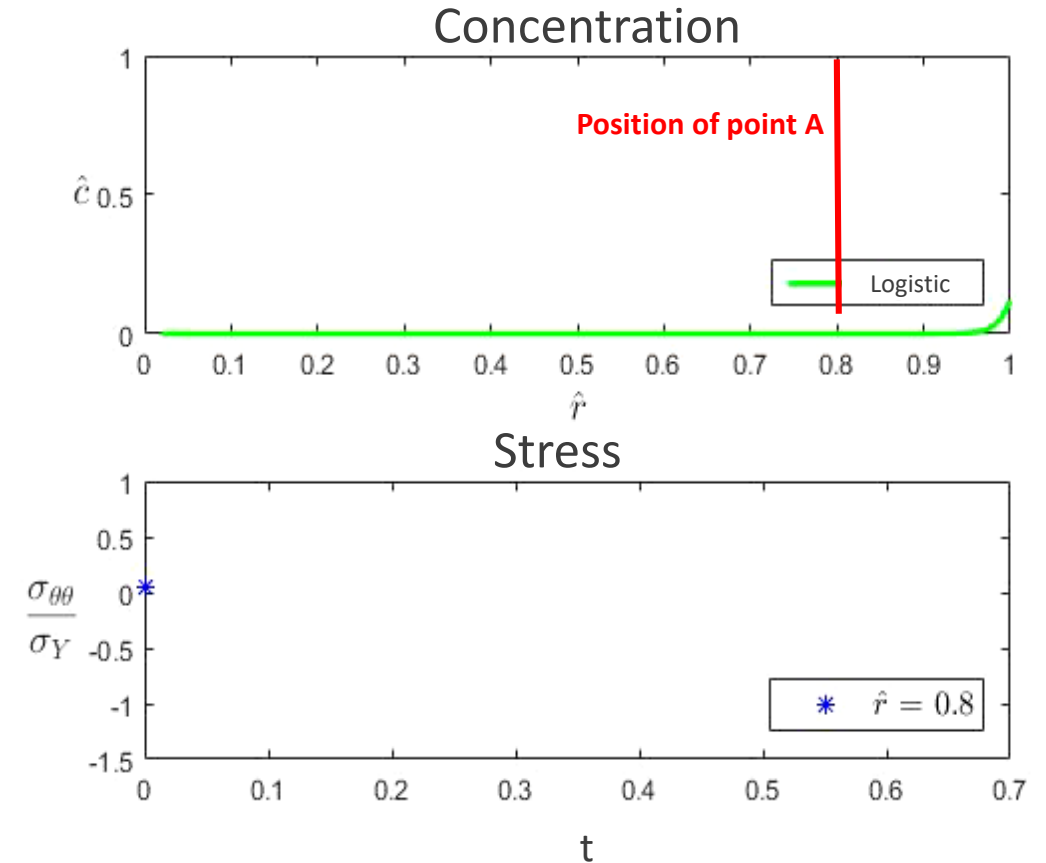
- Using the (13), when $r \rightarrow 0 \rightarrow \sigma_S(0, t) = 0$

- One obtain a system of two nonlinear equations (instead of a single equation as in Seck et al. 2018).

C – Pushing out effect :



(S.Huang et al., Acta Materialia 61 (2013))



Conclusions:

- Stresses are relaxed by plasticity on the lithiation front (Huang et al. 2013).
- Tension on the periphery point (Pushing out effect).